5-2014

Application of High-Performance Liquid-Chromatography Mass-Spectrometry Platform to Study Metabolism and Epigenetic Control of Metabolism

Kylie Patricia Mitchell
Dominican University of California

https://doi.org/10.33015/dominican.edu/2014.bio.07

"Application of High-Performance Liquid-Chromatography Mass-Spectrometry Platform to Study Metabolism and Epigenetic Control of Metabolism"

A Thesis Submitted to the Faculty of
Dominican University of California
&
Buck Institute for Research on Aging
In Partial Fulfillment of the Requirements
For the Degree

Master of Science
In
Biology

By:
Kylie Patricia Mitchell
San Rafael, California
May, 2013

CERTIFICATION OF APPROVAL

I certify that I have read Application of High-Performance Liquid-Chromatography Mass-Spectrometry to Study Metabolism and the Epigenetic Control of Metabolism by Kylie Patricia Mitchell, and I approved this thesis to be submitted in partial fulfillment of the requirements for the degree: Master of Sciences in Biology at Dominican University of California and the Buck Institute for Research on Aging.

Dr. Arvind Ramanathan May 20, 2013
Graduate Research Advisor
Assistant Professor

Dr. Dorn Carranza May 20, 2013
Second Reader

Dr. Kiowa Bower May 20, 2013
MS Biology Thesis Coordinator

Abstract:

Naturally occurring small molecules (metabolites, signaling intermediates) are a critical component of the information flow in biology, along with DNA, RNA, and proteins. Metabolomics is an analytical approach that seeks to comprehensively analyze naturally occurring small molecules and quantify their dynamic changes in biological systems. In recent years metabolomics has begun to provide understanding of the metabolic basis of different diseases, such as heart disease, cancer, and diabetes.

Our lab built a High-Performance Liquid-Chromatography Mass-Spectrometry (HPLC-MS) based metabolomics platform to analyze metabolites from mammalian cells, spent cellular media, and model organisms such as *C. elegans*. We used *C. elegans* to elucidate the metabolic changes seen after treatment with Metformin, which is a known activator of the AMPK pathway.

Cancer cells exhibit high levels of glycolysis producing large amounts of lactate; circumventing the mitochondrial pathway. This phenomenon is known as the Warburg effect. We hypothesize that cancer metabolism is epigenetically regulated. Epigenetics refers to inheritable traits that are not due to alterations in the primary DNA sequence. DNA methylation is an important epigenetic modification. DNA methylation mainly occurs in the CpG islands of the promoter region of genes. It is believed that during cancer development *de novo* DNA methyltransferases methylate tumor-suppressing genes allowing cancer cells to proliferate uninhibited. There are two *de novo* DNMTs, DNMT3A, and DNMT3B. These DNMTs establish the pattern of methylation. We examined *de novo* DNMT-mediated control of cellular metabolism, identifying global

changes in metabolism, as well as differential sensitivity towards glycolytic and mitochondrial inhibitors.

Acknowledgments:

I would like to thank Dominican University of California for giving me the opportunity to pursue a Masters in Biology, and The Buck Institute for Research on Aging.

I would like to give a special thanks to Dr. Arvind Ramanathan, Dr. Sibdas Ghosh, Alexander Patent M.S., Dr. Sonnet Davis, Dr. Samiha Mateen, Dr. Gordon Lithgow, Dipa Bhaumik, Jill Graham, Dr. Silvestre Alavez, Dr. Brad Gibson, Dr. Birgit Schilling, Dr. Deepak Lamba, Dr. Victoria Lunyak, Dr. Christopher Benz, Mariya Yevtushenko, Ultragenyx- Jaclyn Cadaoas

I would also like to thank Theodore, James and Emei Mitchell, Janet Engelhardt, Benjamin Engelhardt, Nesha and Jennifer Elmer, Louise Mitchell, Hayden Kennerley Mesha Kennerley, Royce Kennerley, Tammi Foreman, Steve Shepherd, Betsy Shepherd, Matt Shepherd, Cameron Shepherd, and Jared Greninger for all of their love and support

Table of Contents

Abbreviations:

ACN- Acetonitrile
AdoMet- S-Adenosyl Methionine
A.M.- Agilent Mix
APCI-MS- Atmospheric-Pressure Chemical Ionization
C. elegans- Caenorhabditis elegans
CE- Capillary Electrophoresis
DNMT- DNA Methyltransferase
DPBS- Dulbecco's Phosphate-Buffered Saline
EIC- Extracted Ion Chromatograph / chromatogram
FUdR- 5-fluorodeoxyuridine
GC- Gas Chromatography
HILIC- Hydrophilic Interaction Liquid Chromatography
HPLC-MS- High Performance Liquid Chromatography Mass Spectrometry
LB- Luria Broth
MeOH- Methanol
MTase- methyltransferase
NGM- Nematode Growth Medium
NH_2- Amino propyl
NPLC- Normal Phase Liquid Chromatography
OSHA- Occupational Safety & Health Administration
Q-TOF-Quadrupole Time-of-Flight
RPLC- Reverse Phase Liquid Chromatography
siNT- siGENOME Non-Targeting siRNA
siRNA- small interfering RNA
TIC- Total Ion Chromatograph / chromatogram
TSG- Tumor Suppressing Genes

Chapter 1: Developing an HPLC-MS based metabolomics platform to characterize metabolism In Vitro

Introduction:

Metabolomics is an emerging field of study that seeks to systematically identify and quantify naturally occurring small molecules in a complex biological system. The field of metabolomics compliments the other "omic" fields such as proteomics, transcriptomics, and genomics. The central dogma of biology states DNA is transcribed into RNA, and then RNA is translated into proteins. Cellular biochemicals are a central component of biology, and mediate the flow of information in the central dogma. Cellular metabolites are biochemicals with low molecular weight (<1,800Da) including lipids, amino acids, peptides, nucleic acids, organic acids, vitamins, thiols, and carbohydrates. The analysis of these naturally occurring biochemical allows the metabolic status of a biological system to be defined (Zhou et al., 2012). Metabolism is a complex process that can be broken into two complementary reactions, anabolism and catabolism. Anabolism is the synthesis of large molecules from smaller molecules, and catabolism is the breakdown of large molecules into smaller molecules. Metabolism is a systemic reaction occurring in every tissue and cell of an organism all of the time. Metabolomics has two different but complementary analytical of approach-targeted and untargeted. When approaching metabolomics in a targeted fashion identification and quantification of specific metabolites or metabolite classes in a particular pathway is the focus of study. A targeted approach is therefore hypothesis driven. An untargeted approach seeks to identify all metabolites in a biological system, this approach is generally used to further develop a hypothesis, an untargeted approach is more discovery based. Metabolomics is currently being developed to identify biomarkers; in response to environmental stress, drug discovery, comparing mutants, toxicology, nutrition, studying global effects of genetic manipulation, cancer, comparing different growth stages,

diabetes and natural product discovery (Zhang et al., 2012a). The range of chemical properties of these different small molecules is diverse and therefore requires the appropriate separation technique to analyze metabolites.

A wide variety of analytical approaches must be employed in metabolomics analysis. There are multiple highly validated instruments used to study metabolism. Of the different instruments available that are accepted to produce high quality, reproducible results include but are not limited to NMR, MS, GC-MS, HPLC-MS, CE-MS, and UPLC-MS. These methods will briefly be discussed.

Nuclear Magnetic Resonance (NMR) uses the magnetic properties of certain nuclei creating magnetic dipole and quadrapole moments (Kleckner and Foster, 2011). NMR is one of the most common spectroscopic analytical techniques because it has the ability to identify and quantify a wide range of organic metabolites. NMR-based metabolomics provides a real-time analysis of metabolites allowing one biological sample to be used in a time course without disrupting the sample itself. However, NMR has a relatively low sensitivity threshold when measuring metabolites, making it an inadequate method for measuring low-abundance metabolites (Zhang et al., 2012a).

Mass Spectrometry (MS) is a method of analyzing metabolites that can either be performed on its own, or coupled with another analytical technique such as chromatography. MS has gained prominence because of its high sensitivity, and wide range of detectable metabolites. MS has also proven to be reliable, reproducible, and high-throughput (Lei et al., 2011). A mass spectrometer is comprised of three main parts; ion source, mass analyzer, and detector. The ion source first converts sample molecules into ions, depending on the mass analyzer, ions are either resolved in a time-of-flight tube or in an electromagnetic field, then metabolites are measured by

the detector (Zhou et al., 2012). Direct injection is not an ideal method to examine complex mixtures and identifying individual metabolite peaks because of the possibility of ion suppression and the matrix effect (Gosetti et al., 2010), however MS fingerprinting is still a useful tool in examining patterns of metabolites. Fingerprinting is also useful when trying to distinguish between two different physiological states (Allen et al., 2003).

For higher resolution of metabolites a common practice has been to couple MS with chromatography. Gas Chromatography (GC) is a common analytical technique used in plant metabolomics. GC provides an ideal profiling approach to analyzing polar and non-polar metabolites, especially lipid metabolites. Polar metabolites are derivatised to render them volatile. If a metabolite is not volatile it cannot be detected by GC. Polar metabolites require derivitization at a functional group such as hydroxyl (-OH), sulfhydryl (-SH), and carboxyl (-COOH), etc. This is to reduce polarity, and increase thermal stability and volatility (Dettmer et al., 2007; Zhang et al., 2012a). Common derivitization methods include alkylation, acylation and silylation. Alkylation reagents reduce the polarity of the compounds by substituting aliphatic or aliphatic-aromatic group for labile hydrogens. Acylation removes the labile hydrogens and transforms the compound into an ester, thioester, and amides. These two methods require a purification step before analyses on the GC (Schummer et al., 2009). Silylation is another common derivatization method in which the labile hydrogens from acids, alcohols, thiols, amines, amides or enolizable ketones and aldehydes are replaced by a trimethylsilyl group, this reaction occurs via nucleophilic attack (SN_2). Common silylation reagents are N, O-bis-(trimethylsilyl)trifluoroacetamide (BSTFA), and N-methyl-trimethylsilyltrifluoroacetamide (MSTFA) (Schummer et al., 2009). The advantage of using GC is typically that it can be coupled to a single quadrupole instrument and uses Electron Ionization (EI). The advantages of an EI are

a low influence of molecular structure on response, and a large number of characteristic fragments. The disadvantage is the derivitization process and the necessity of metabolites to have labile hydrogens that can undergo derivatization (Alder et al., 2006).

Capillary Electrophoresis (CE) is a method of separation. CE separates analytes with high resolution based on their migration through a liquid filled capillary column in an electric field. Capillary Electrophoresis-Mass Spectrometry (CE-MS) is a favorable method of identifying polar or ionic compounds found in biological samples, including urine, blood, and saliva. CE-MS is also used to analyze inorganic ions, organic acids, amino acids, nucleotides and nucleosides, vitamins, thiols, carbohydrates, and peptides (Metzger et al., 2009; Zhang et al., 2012a). A disadvantage of CE-MS is that in order to achieve unidirectional movement of analytes the electrophoretic separation must be done in an electric field. This makes it difficult to couple CE to the ion source of an MS. Decreasing the electric field is possible, however this action reduces efficiency and resolution (Heiger, 2000).

A method that has been extensively developed for metabolomics analysis is high performance liquid chromatography coupled to mass spectrometry (HPLC-MS). HPLC-MS separates metabolites through a column in one of two ways, isocratic or gradient elution. Isocratic elution uses a water-solvent composition that remains constant during the metabolite separation. Isocratic elution is common when a sample contains approximately 10 metabolites. The other method is a gradient elution, which uses a gradient of solvents over a time course, based upon the composition of the buffers, metabolites with similar chemical properties will elute. Gradient elution creates narrow metabolite peaks, and faster analysis (Zhou et al., 2012). HPLC-MS allows semi-polar and polar metabolites to be identified. The spectrum of chemical properties observed in metabolomics prevents any one column from identifying all metabolites,

therefore a variety of columns and chemistries must be employed. Hydrophilic Interaction Liquid Chromatography (HILIC) is the ideal method for separating amino sugars, amino acids, vitamins, carboxylic acids and nucleotides (Buszewski and Noga, 2012; Xiao et al., 2012). HILIC also compliments Reverse Phase LC (RPLC), allowing compounds that are not sufficiently retained under RPLC conditions to be resolved by giving an opposing elution of metabolites to that of RPLC. Normal-Phase LC (NPLC) can also separate polar compounds, however NPLC is more compatible with APCI-MS instead of ESI-MS. HILIC can use any polar stationary phase. A commonly used stationary phase is an amino-propyl stationary phase (Xiao et al., 2012). The mobile phase consists of a mixture of water-water miscible organic solvents, usually acetonitrile. Starting with a high percentage of organic solvent non-polar metabolites are able to elute from the column. Gradually increasing water or aqueous content allows polar metabolite elution from the column (Greco and Letzel, 2013). HILIC is different from both normal phase, and reverse phase LC with characteristics of both methods.

Our lab specifically uses an Agilent HPLC, which directly injects samples into an Agilent 6520 Accurate Mass Quadrupole Time-Of-Flight (TOF) System. This system has a mass accuracy of 0.001 amu. Since metabolites of interest have an average mass of ~1,000 Da identifying metabolites using this system reduces the possibility of formulae. In Figure 1 the orange bar denotes the mass accuracy of this system. Metabolites of interest are typically <1,000 Da which means that an identified metabolite has approximately 10 possible chemical formulae. This prevents the necessity of fragmenting large quantities of standards to eliminate potential formulae of metabolites.

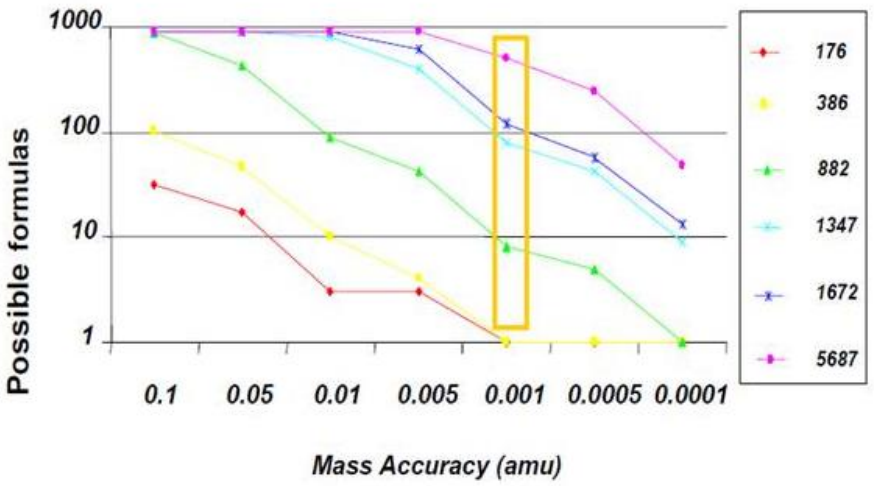

Figure 1: Mass accuracy vs. theoretically possible chemical formulae. The Orange bar denotes the mass accuracy of the Agilent 6520 Q-TOF; metabolites of interest are typically ≤ 1000 Da, this allows approximately 10 possible chemical formulae per metabolites.

Materials and Methods:

Extracellular Metabolite Extraction:

1 ml of culture medium was collected from each sample for extracellular metabolite extraction. Samples were centrifuged for 10 minutes at 15,000 x *g* and at 4°C to remove cell debris. If samples were not processed immediately, they were placed at -80°C. 400 µL of sample was placed in a glass vial containing 400 µL of 100% MeOH +0.1% Agilent Mix (AM). AM is a mixture of two known metabolites with distinct peaks and abundances. Solvents are spiked with a known concentration, when samples are run on the MS we use these peaks to ensure the abundance is equal across all samples, as well as ensuring the retention time is the same. This ensures the HPLC is running properly. Non-polar metabolites were extracted by adding 800 µL of $CHCl_3$ was spiked with 0.1% fatty acid standard. The samples were centrifuged at 3,000 x *g* for 10 minutes. Forming two distinct layers, separated by a thin white film, this is debris that has

precipitated out and will not be further analyzed. The top layer, MeOH, contains the polar metabolites. The lower organic layer, $CHCl_3$ contains the non-polar lipid metabolites which were removed using a glass pasture pipette and dried using liquid nitrogen (LN_2). The polar metabolites in MeOH were dried down using a SpeedVac. Polar metabolites were reconstituted in 100 µL of 50% MeOH and nonpolar metabolites were reconstituted in 100 µL of $CHCl_3$, before being run on the HPLC-MS. Any remaining sample was placed at -80°C.

Intracellular Metabolite Extraction:

Cells were washed twice with cold 1X PBS in order to remove any residual media or extracellular components and then lysed using 400 µL 50% MeOH + 0.1% A.M. when plated in a 6-well dish. The cells were scraped and collected into a 9ml glass separation vial. Samples were centrifuged at 3,000 x *g* for 10 minutes at 4°C, forming two distinct layers. The top layer contains the polar metabolites. The lower organic layer contains the non-polar lipid metabolites. The lower organic layer was removed and dried using LN_2, and the polar metabolites, in MeOH, were dried down using a SpeedVac. Polar metabolites were reconstituted in 100 µL of 50% MeOH, and the nonpolar metabolites were recinstituted in 100 µL of $CHCl_3$. Remaining samples were stored at -80°C.

Extracellular MS Fingerprinting:

Spent media was used to detect extracellular metabolites. The samples were then diluted ten-fold. Aliquot 5µl of media and combine that with 50µl of 30% MeOH+0.1% ammonium hydroxide. Samples were then centrifuged at 8,000 x *g* for 5 minutes at 4°C. 30µl of sample was then transferred to an auto-sampling vial and directly injected into the MS.

High Performance Liquid Chromatography-Mass Spectrometry:

Performance of LC-MS was accomplished using an Agilent 1200 series HPLC system and a G6520 accurate mass Q-TOF high resolution mass spectrometer. Data was acquired from 10µl injections of each sample employing a 35 minute gradient at a flow rate of 0.3ml/minute. A HILIC gradient was employed, which includes two solvents: A. 20 mM Ammonium Acetate (NH_4OAc) + 5% Acetonitrile (ACN) and B. ACN. Solvent gradients are listed in Table 1. Total time per HPLC run is 47 minutes.

Table 2: Solvent Gradient

Time (minutes)	% A	% B
0	5	95
25	90	10
30	90	10
30.1	5	95
30	5	95

Table 2: Solvent Gradient for HILIC chromatography. A - 20 mM NH_4OAc + 5% ACN, B - ACN

The conditions of the column include: a Luna amino propyl (NH_2) column (150 x 2.0 mm 3µm) held at 20°C, purchased from Phenomenex. Data was acquired over a mass range of 100-1100 Daltons in negative ion mode, and data analysis was conducted using Agilent MassHunter version B.04.00 and Mass Profiler Professional version B.12.

Results and Discussion

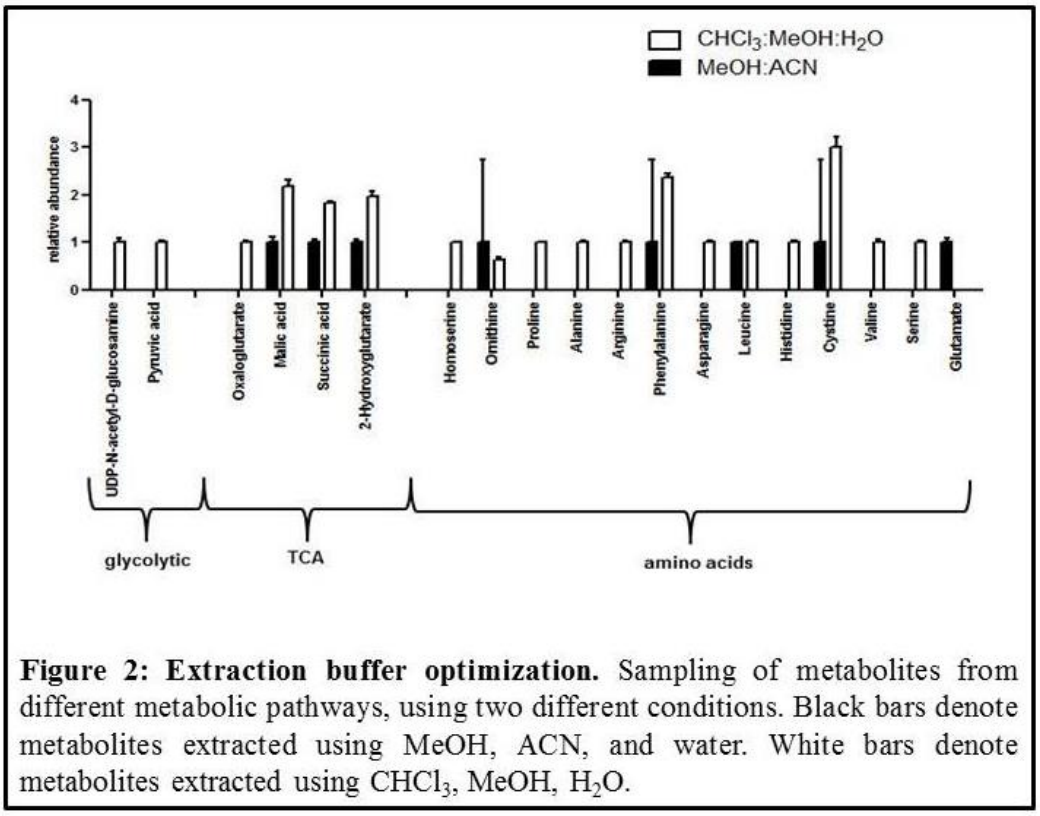

Figure 2: Extraction buffer optimization. Sampling of metabolites from different metabolic pathways, using two different conditions. Black bars denote metabolites extracted using MeOH, ACN, and water. White bars denote metabolites extracted using $CHCl_3$, MeOH, H_2O.

The method of extraction first designed in our lab was taken directly from the Rabinowitz lab at Princeton University. At this lab, extractions using varied solvents, and varying amounts were performed. A method of combining acetonitrile/ methanol/ water (40:40:20) with their samples and then placing this mixture at -20°C for 15 minutes, removing the supernatant, and adding additional solvent to re-extract metabolites was described (Rabinowitz and Kimball, 2007). When using this method of extraction we were able to detect a range of metabolites; however the life of the HPLC column was short-lived. The extraction method above was causing large molecules to clog the separation column and guard column. Figure 2 shows a small sampling of metabolites from different metabolic pathways that were detected after extracting neural stem cells. Due to the premature decline of the column, we went back into the literature

and discovered an alternative method of extraction, employing a 1:1:3 H_2O; MeOH; $CHCl_3$ mixture (Sana and Fischer, 2009). After performing the two extraction methods side by side, we are able to identify more metabolites using chloroform in the extraction.

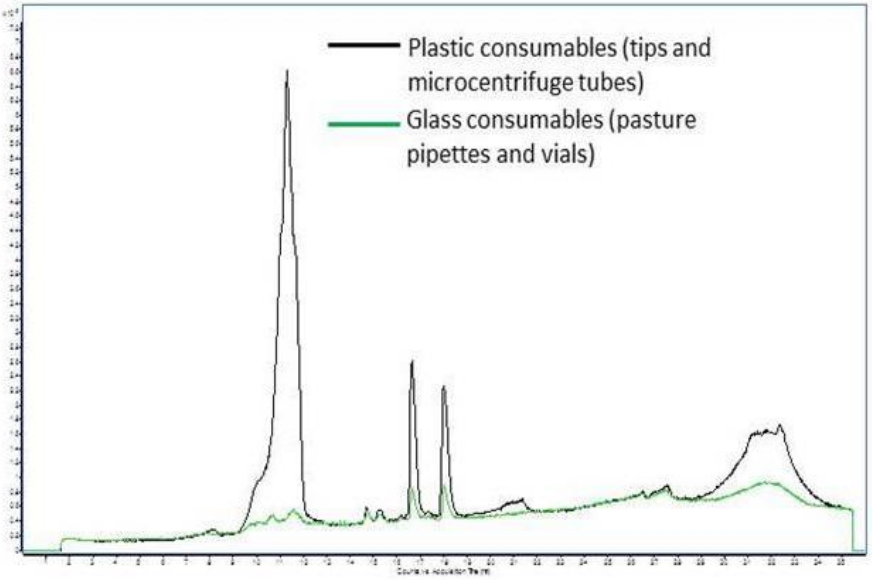

Figure 3: Optimization of metabolite extraction in plastic vs. glass consumables. The black Total Ion Chromatogram (TIC) denotes samples prepared using plastic tubes and tips, the green TIC denotes samples prepared using all glassware.

After determining the chloroform method was more advantageous in terms of quantities of identified metabolites, and less error among biological replicates optimization trials of multiple parameters was conducted. To ensure no artificial peaks were being detected optimization trial solidified the notion that plastic is highly incompatible with chloroform. Figure 3 shows the comparison of two Total Ion Chromatograms (TIC); the extractions were performed side by side of two control samples of neural stem cells. Sample conditions were consistent, the only variable was plastic or glass consumable products. The green line denotes samples that were

extracted using glass vials, and glass pasture pipettes, where the black line represents that extraction performed using autoclaved microcentrifuge tubes, and autoclaved plastic pipette tips.

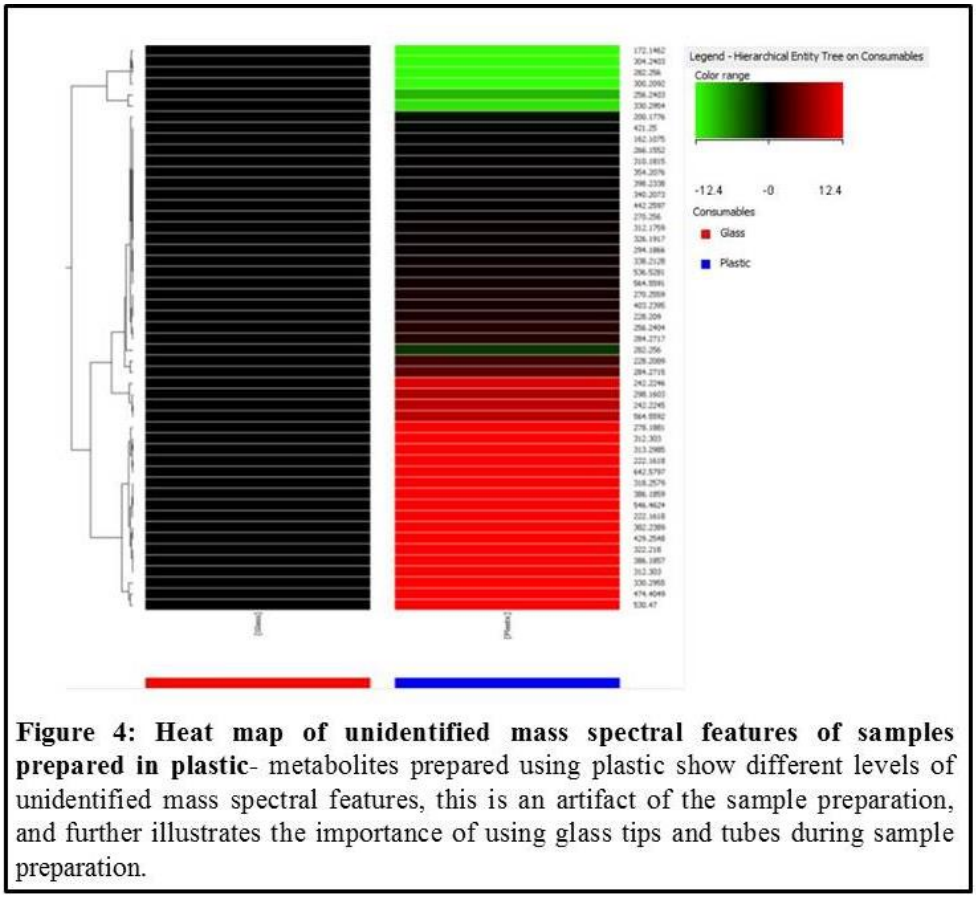

Figure 4: Heat map of unidentified mass spectral features of samples prepared in plastic- metabolites prepared using plastic show different levels of unidentified mass spectral features, this is an artifact of the sample preparation, and further illustrates the importance of using glass tips and tubes during sample preparation.

Use of plastics with chloroform can indeed cause artificial peaks to appear. After data analysis a heat map of various unidentified mass spectral features shows large variation between glass consumables and plastic consumables. Figure 4 is a heat map of unidentified mass spectral features that are either up or down-regulated. The only experimental condition that was different was the use of glass or plastic. This leads us to believe that chloroform is allowing plasticizer molecules to leach into the samples causing these contaminating peaks. All steps that include the use of chloroform are performed in glassware only, as to prevent these artificial peaks. OSHA guidelines, regarding the storage and use of chloroform, clearly states “Do not use rubber or plastic hose or pipe to transfer chloroform” (Administration). leading us to believe the best

approach would be to use chloroform in glassware, preventing the chloroform from leaching plastics into samples, and the HPLC/MS.

Conclusions:

Developing a method necessitates intense literature searches. All aspects starting from sample preparation to conducting statistical analysis of metabolites after data analysis is completed is a time-consuming process. Once an analytical technique has been developed, and metabolites can successfully be identified, samples from a wide range of biological applications can be examined. This is not to say that once a satisfactory method has been developed no other methods should be examined. Therefore, as different methods become available they may be viewed as alternatives.

Chapter 2: *Caenorhabditis elegans*- a model organism to examine the interaction between *ahr-1* and Metformin.

Introduction:

The Aryl Hydrocarbon Receptor (AHR) pathway is known for its importance in development, and its role in dioxin mediated cytotoxicity.(Nebert et al., 2000) AHR is a basic helix-loop-helix (bHLH) and Per-Arnt-Sim containing transcription factor that is ligand-dependent (Nguyen and Bradfield, 2008) .Figure 5 shows these different domains in murine model, the Ala375 position has been identified as a polymorphism that is responsible for ligand affinity. When $Ala_{375} \rightarrow Val_{375}$ ligand affinity is greatly reduced.

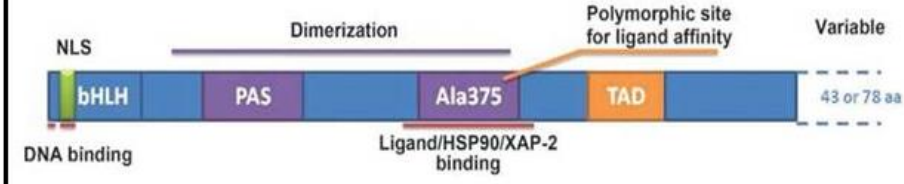

Figure 5: Protein domains in the mammalian Aryl Hydrocarbon receptor (Zhang, 2011). AHR is a basic helix-loop-helix (bHLH) and Per-Arnt-Sim (PAS) containing transcription factor that is ligand-dependent, Ala375 has been identified as a polymorphism that reduces ligand affinity.

AHR has many high affinity ligands including a wide variety of ubiquitous and hydrophobic environmental contaminants such as halogenated aromatic hydrocarbons (HAHs) and non-halogenated polycyclic aromatic hydrocarbons (PAHs). The most well characterized HAHs is 2, 3, 7, 8-tetrachlorodibenzodioxin (TCDD) which is the most potent known agonist of AHR (Denison et al., 2002). While AHR was discovered for its importance in dioxin binding, it gained much interest when it was discovered to play a role normal physiology and development (Zhang, 2011). In AHR null mice many developmental issues arose, the portcaval shunt in the

developing liver failed to close immediately causing hepatovascular blood flow and altered disposition of small molecules requiring hepatic clearance. Mice also experienced other vascular issues including the persistence of the hyaloid artery and an altered limbal vasculature within the developing eye. This led to the conclusion that AHR plays an important role in the regulation of normal vascular or hematopoietic development (Nguyen and Bradfield, 2008). Mice carrying the hypomorphic AHR allele experienced the same developmental issues. These mice could be rescued by TCDD treatments. The ductus venosus closed properly after this activation, which suggests this is an endogenous function of AHR (Zhang, 2011). Non-ligand bound AHR is located in the cytoplasm in an inactive protein complex composed of a dimer of Heat Shock Protein 90 (Hsp90), prostaglandin E synthase 3, and a single molecule of the immunophilin-like protein hepatitis B virus X-associated protein 2 (XAP2). Figure 6 is a schematic representation of a ligand binding to AHR. Upon ligand binding the XAP2 is released, then ligand bound AHR translocates to the nucleus and dissociate from the remaining protein complex, exposing the PAS domains, which allows the Aryl Hydrocarbon Receptor Nuclear Translocator (ARNT) to bind AHR. This heterodimer complex then directly and indirectly interact with DNA by binding to the 5' regulatory region of dioxin-responsive genes (Zhang, 2011). AHR has been referred to as an "environmental sensor" because of its ability to bind to and metabolize environmental toxins (Nguyen and Bradfield, 2008). Understanding cellular metabolism of environmental stimuli is crucial in understanding how the environment alters gene transcription, metabolism, and other physiological functions. Because the levels of metabolites can be regarded as the ultimate response of biological systems to genetic or environmental changes, coupling it to transcriptomics and proteomics allows for a more comprehensive understanding (Ma et al., 2012).

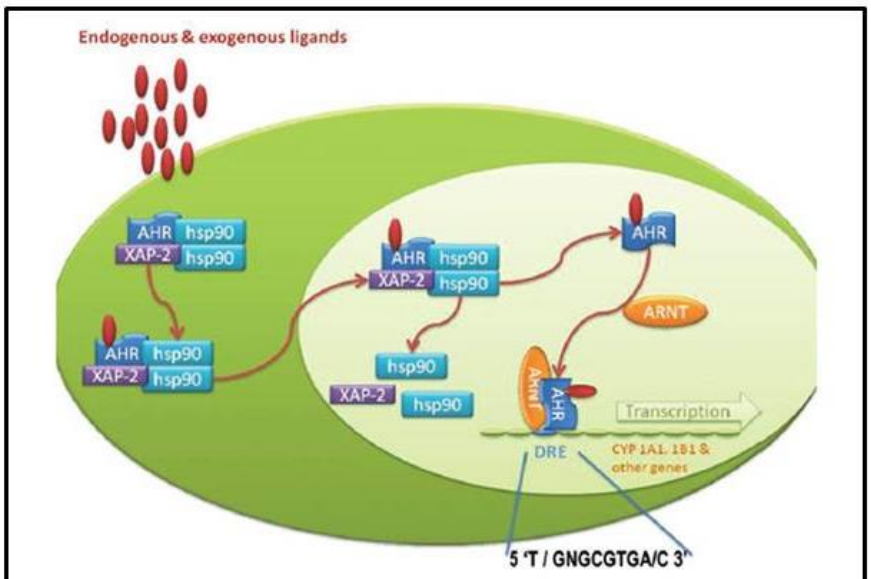

Figure 6: Aryl Hydrocarbon receptor signaling pathway (Zhang, 2011). Ligand bound AHR translocates into the nucleus. The chaperone complex dissociates and AHR binds to ARNT creating a heterodimer and transcription of dioxin-response genes occurs.

Caenorhabditis elegans (*C. elegans*) are free-living soil nematodes. *C. elegans* have a defined lifespan of approximately 3 weeks, including a 3 day larval period. *C. elegans* were the first multicellular organism to have their entire genome sequenced. Along with their transparency, hermaphroditic nature *C. elegans* genetics are also easily manipulated via RNAi, or creating gene knockout mutant strain (Frooninckx et al., 2012). All of these factors make *C. elegans* powerful model organisms. AHR is conserved in *C. elegans*, the ortholog is termed *ahr*-1, and the nuclear dimerization partner is encoded by *aha*-1. *Ahr-1* and *aha-1* has been directly implicated in the differentiation of neurons, more specifically the AVM and SDQR. *C. elegans* have a surprising resemblance as far as their nervous system is concerned to vertebrates (Frooninckx et al., 2012). When *ahr-1* is knocked down, strains showed reduced growth, reproduction, and survival. Defects in other systems have also been reported including the liver,

heart, ovaries, and the vascular and immune system (Qin and Powell-Coffman, 2004). There are multiple *ahr-1* knock out worms ZG24 and CZ2485. The ZG24 strain is a deletion of 1165 base pairs which includes multiple exons in the PAS domain. The CZ2485 strain is a substitution of one nucleotide (c/t) (wild type/ mutant) causing a premature stop codon in the *ahr-1* protein (WormBase). *C. elegans ahr-1* mutants are valuable *in vivo* models. Although there may be differences between the mammalian and *C. elegans ahr-1* ortholog certain similarities can shed light on the mammalian counterparts. Determination of pathway interactions could allow for further understanding regarding cross talk between different pathways of interest. The AMPK pathway is another pathway that is conserved in *C. elegans*. Metformin, 1, 1-Dimethylbiguanide hydrochloride has been shown to have a lifespan extending phenotype through activation of the AMPK pathway. The AMPK pathway has been dubbed the energy sensing pathway, however how it senses an environmental cue is still unknown. Determining the relationship between Metformin, the AHR pathway and AMPK pathway may help understand how environmental cues affect metabolism. Utilizing *ahr-1* knockout worms and Metformin, we can examine cross talk of AMPK-AHR pathways.

Materials and Methods:

Strains and Culturing:

The *ahr*-1 mutant strains - CZ2485 and ZG24 - were ordered from Caenorhabditis Genetics Center (CGC). The Bristol N2 strain a kind gift from Dr. Gordon Lithgow (Buck Institute) served as a control. Worms were cultivated and maintained on nematode growth medium (NGM) plates with OP50 as a food source.

Lifespan Assay:

For the first seven days of the lifespan the worms were placed on 5-fluorodeoxyuridine (FUdR) (+) plates to prevent the eggs from hatching. The final concentration of FUdR is 10 µg/mL. Metformin (Sigma-Aldrich St. Louis, MO) was added at varying concentrations, 50 mM, and 25 mM. 30-40 L4 worms were placed on each plate Worms are counted every 2-3 days during the experiment; the dead worms are tallied. As the lifespan continues the worms will begin to move less frequently. During lifespans, platinum wire should be used to gently prod the worm on the head if the worm does not respond to the prod they are considered dead. Worms were censored if they crawled off the plate, suffered from internal hatching, or protrusion of gonads was observed. The lifespan data were plotted on a survival curve using Graphpad Prism 4.

Mass Cultures:

When mass culturing worms, OP50 must be concentrated. Place 25 g of Luria Broth (LB) into a 2L flask. Add 1L of nanopure water, autoclave the solution, once the solution has cooled inoculate the LB with 10µl of OP50. Allow the bacteria to grow for 16 hours. Once the cultures become cloudy centrifuge at 3,000 RPM for 1 hour, remove the supernatant and resuspend the bacteria, for every liter of bacteria ~15 ml of s-basal should be used.

When mass culturing worms, thousands of eggs must be harvested. To obtain this amount of eggs in the same developmental stage, adult worms must be dissolved while keeping the eggs intact. To hypo the worms wash a 10 cm plate with 3 ml of S-basal. Place the worms into a 15 ml conical. Pellet the worms, than add 10 ml of a hypochlorite solution to the worms. The adult carcasses should dissolve after vigorously shaking the conical for ~30 seconds. Once the adult worms have completely dissolved the eggs should be washed 5 times with S-basal to ensure all

the hypochlorite solution is removed. Eggs should be incubated in S-basal overnight to ensure all eggs have hatched and have entered into the L1 stage of development. The L1 worms should be counted and approximately 10,000 L1s should be placed on a 10 cm plate and incubated until they have reached the L4 stage of development. Once the worms have reached the L4 stage they are to be placed on Metformin + FUdR plates, or the control plates containing FUdR. After the appropriate time has elapsed the worms should be collected. To collect the worms place 3 ml of S-basal on the plate and swirl the plate to suspend the worms. Collect the worms into a 15 ml conical; allow the worms to gravity settle for 10-15 minutes, than aspirate off access S-basal. To snap freeze the worms until they are ready to be processed further place the conical in liquid nitrogen until the entire pellet has frozen then immediately place the samples at -80°C.

Metabolite Extraction:

In a 50 ml glass centrifuge vial place the worm pellet, obtaining both the weight of the glass vial, then the weight of the glass vial with the sample. Add 4 ml of ice cold 50% MeOH. Maintain the worms on ice from this point. Subject the culture to 4- 1 minute sonication while on ice. Add 8 ml of chloroform to each sample, vortex the samples vigorously for 30 seconds. Allow the two layers to settle, slowly remove the top aqueous layer of MeOH containing the polar metabolites. Once the aqueous layers have been removed add equal volumes 0.5M KCl/ 0.08M H_3PO_4. Vortex the samples vigorously for an additional 30 seconds, now Place the samples in an ultrasonic water bath for 15 minutes. Samples were vortexed twice in 1 minute intervals. Centrifuge the samples for 2,000 x *g* for 10 minutes to separate the phases. Collect the lower organic layer which contains non-polar metabolites. Samples were dried under nitrogen until all chloroform has been removed.

Results and Discussion

Lifespan of Wildtype N2 and ahr-1 Mutant Worm Treated with 50mM Metformin:

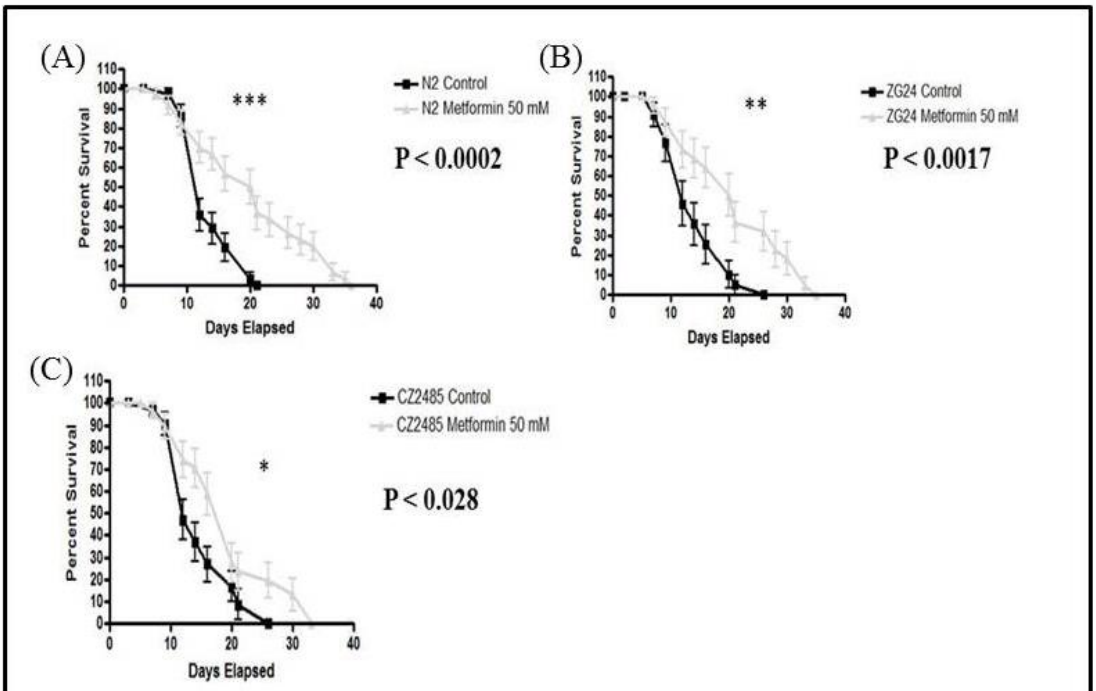

Figure 7: Lifespans of Metformin treated wild-type and mutant strains. (A) shows wild-type worms, treated with 50mM Metformin. (B) *ahr-1* (ZG24 strain) null worms, treated with 50mM Metformin. (C) *ahr-1* (CZ2485 strain) null worms, treated with 50mM Metformin. Black lifespan curves represents control populations, and grey lifespan curves represent Metformin treated.

Lifespans of *ahr-1* null worms in the presence and absence of Metformin were conducted to determine if *ahr-1* influenced Metformin mediated lifespan extension. Figure 7 shows the lifespan of N2 wild-type worms treated with 50 mM Metformin, a dramatic increase in lifespan is seen with the addition of Metformin. *C. elegans* not only experienced an overall extension, but a median extension as well. During the lifespan assay not only was worm death taken into account but worm health-span was also noted. (Data not shown) Metformin worms showed increased mobility later in life, in contrast to respective control worms. Both *ahr-1* mutant worms showed a statistically significant increase in lifespan. Figure 8 is a lifespan comparing the

ahr-1 null Metformin treatment worms to the N2 Metformin treated worms no statistically significant changes occurring.

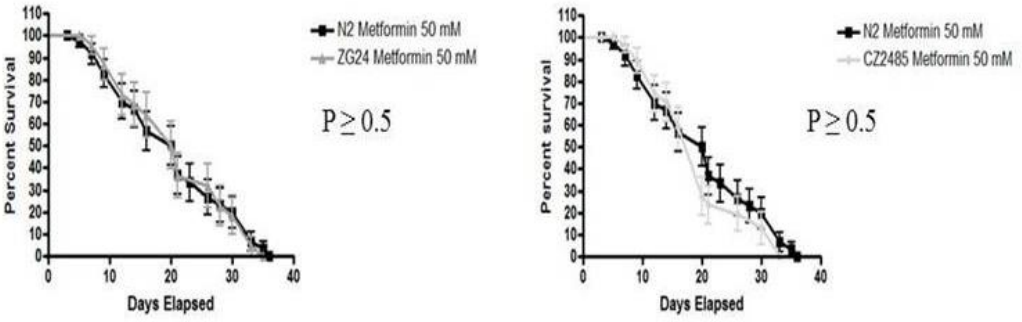

Figure 8: Wildtype *C. elegans* compared to *ahr-1* null *C. elegans* both treated with 50 mM Metformin. (A) Wild-type and *ahr-1* (ZG24) worms show similar lifespan extension when treated with 50mM Metformin. (B) Wild-type and *ahr-1* (CZ2485) worms also show a similar lifespans.

The lifespan analysis of *ahr-1* null worms compared to the wild-type worms showed no median lifespan extension, or overall lifespan extension that was statistically significant. This leads us to believe that Metformin is acting independently of the *ahr-1* gene.

Metabolomics of Metformin Treated C. elegans:

Implementing our untargeted metabolomics based platform as discussed in Chapter 1, a global analysis of polar and non-polar metabolites was conducted. Mass cultures of N2 worms were grown on Metformin plates for 5 days. The goal of extracting metabolites after 5 days is to determine the early metabolism changes that the worms experience while being exposed to 50 mM Metformin.

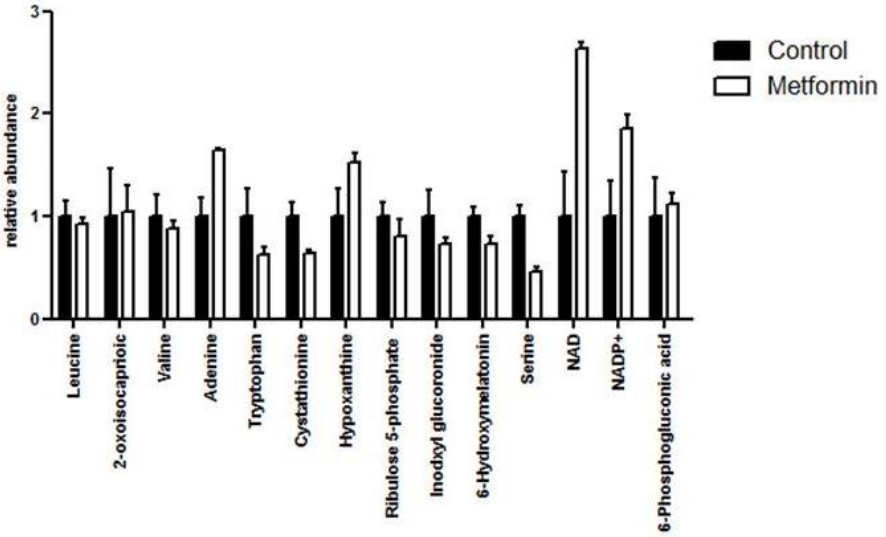

Figure 9: Global Metabolites Identified after metabolomics profiling of *C. elegans*. A number of metabolites were identified to be significantly altered after Metformin treatment. A representative subset of significantly altered metabolites from multiple pathways are listed above.

Figure 9: is a subset of metabolites from an array of different pathways that were found to be significantly altered upon Metformin treatment. From our initial screen of significantly altered metabolites one pathway showed potential. The branched chain amino acid degradation pathway (BCAA) showed three metabolites were significantly altered, leucine, isoleucine, and valine. Further analysis of the BCAA degradation pathway is shown in Figure 10. Analysis of intermediates in the BCAA degradation pathway showed slight increases and decreases, however no additional significantly altered metabolites were identified.

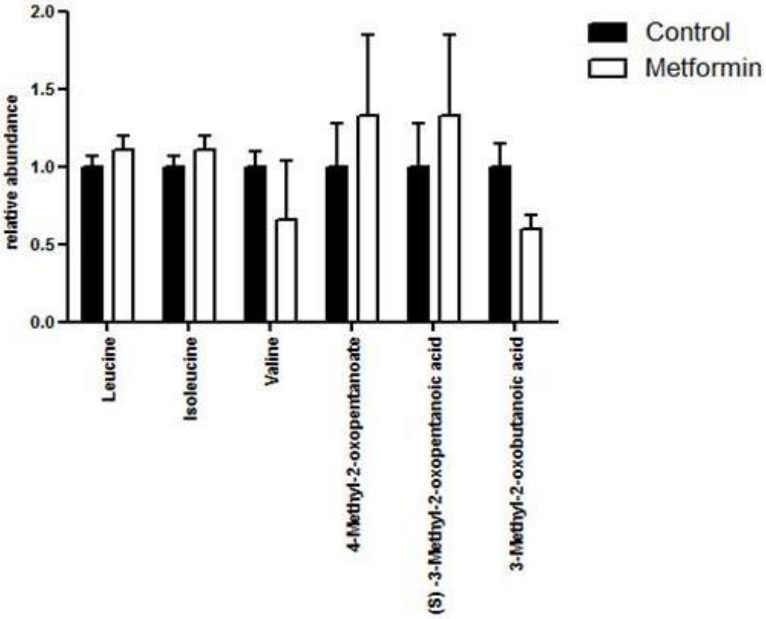

Figure 10: Metabolites in the Branched-Chain Amino Acid pathway identified by metabolomics analysis. Further analysis into the BCAA pathway showed no additional metabolites to be significantly altered.

This pathway could be cooperating with other pathways in mediating Metformin metabolism. Mutant strains lacking enzymes in the branched-chain amino acid pathway can shed more light on the role BCAA's play in Metformin mediated lifespan extension.

Conclusions:

Metformin is an important drug that is currently being used by millions of Americans to combat type II diabetes. The mechanism of Metformin is not fully understood. Our first hypothesis was *ahr-1* was involved in the metabolism of Metformin. When conducting a lifespan using the null worms no significant change was examined. The mechanism of Metformin may be working through multiple pathways, with varied effects in many pathways. A global analysis of all metabolites was conducted to determine if a certain pathway was up or down regulated. This portion of research was not a main focus, therefore we have not completed data mining to

determine if another pathway was significantly altered. Some prospective pathways include NAD metabolism, serine degradation pathway, and tryptophan degradation pathway. Along with mining the current data; future experiments could include more biological replicates, and collection points.

Initially, this data lead us to believe the branched chain amino acid degradation pathway could be the potential target. BCAA degradation pathway has been shown to be important in glucose and insulin sensitivity in mice that were fed a high fat diet (Newgard et al., 2009). The data that was collected suggests that the mechanism by which Metformin works could be the BCAA degradation pathway in cooperation with other pathways.

Chapter 3: DNA Methyltransferase Mediated Regulation of Cellular Metabolism

Introduction:

Epigenetics is a term that refers to the reversible, inheritable trait (e.g. gene expression) wherein the DNA sequence itself is not altered. DNA methylation is an example of epigenetic modification that mainly occurs at the C5 position of cytosine (5mC) within a CpG island. CpG islands are short regions of DNA ranging from 0.5-4kb in length that is often found in the promoter regions of genes. The donor methyl group comes from S-Adenosyl methionine (AdoMet). The process of DNA methylation as seen in Figure 5 is carried out by DNA Methyltransferases (DNMTs). These enzymes catalyze the covalent addition of a methyl group from AdoMet to the 5 position of the cytosine ring (Fukushige and Horii, 2013). DNA methylation can be inhibited by the compound 5-azacytidine, which contains a nitrogen in the cytosine ring at the 5 position. This forms a covalent bond between the 5-azacytidine and the DNMT (Fukushige and Horii, 2013).

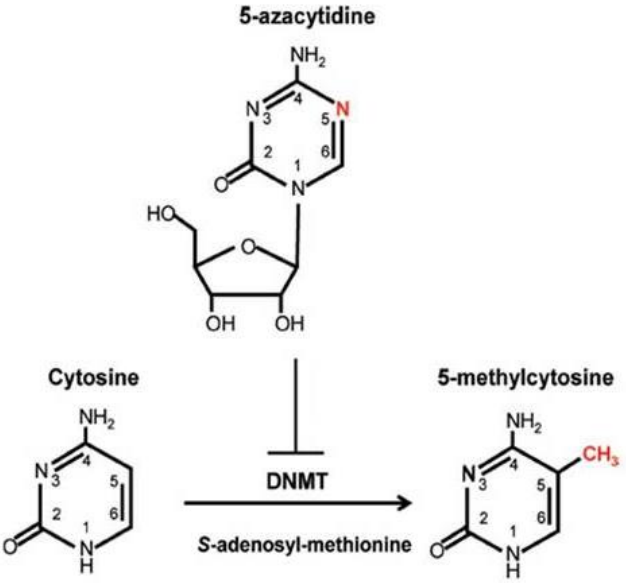

Figure 11: Methylation of cytosine by DNMTs and inhibition of methylation by 5-azacytidine (Fukushige and Horii, 2013). DNMTs catalyze the covalent addition of a methyl group from AdoMet on the 5 position of the cytosine ring. DNA methylation can be inhibited by 5-azacytidine, which contains a nitrogen in the cytosine right at the 5 position. A covalent bond is formed between the 5-azacytidine and the DNMT

Methylation of DNA plays an especially important role during early embryonic development, stem cells differentiation, and tissue-specific gene expression (Yim et al., 2012). However, DNA methylation also plays a significant role in the development of many different forms of cancers (Liu et al., 2007; Yan et al., 2011). In tumor cells, unlike normal cells, a high proportion of CpG islands are hypermethylated, thereby silencing specific genes, such as tumor suppressing genes (TSG). Hypermethylation of the TSGs is one of the most well-categorized epigenetic events in tumor formation (Jones and Baylin, 2002). For example, hypermethylation of the promoter region of the BRCA1 gene has been shown to lead to breast cancer and hypermethylation of STK11 genes have been linked to familial forms of renal, breast and colon cancer (Jones and Baylin, 2002). Along with TSGs being hypermethylated, cancer cells also exhibit demethylation of oncogenes during the development of cancer. For example, certain

carcinogens, such as cigarette smoke extract (CSE) have the ability to downregulate the DNMT isoform DNMT3B, which leads to demethylation of oncogenes (Liu et al., 2007). Recent studies have shed light upon demethylating enzymes. The TET family of genes has specifically TET1, TET2, and TET3 has been gaining increased attention because they demethylated mammalian DNA (Tsumagari et al., 2013).

There are two different families of DNMTs, DNMT1, and 3. Figure 12 is a schematic of DNMTs, DNMT1 is a maintenance enzyme that is responsible for maintaining methylation patterns during chromosomal replication and repair by associating with replication sites by directly binding to proliferating cell nuclear antigen. The newly synthesized strand of DNA now contains the same DNA methylation pattern (Mortusewicz et al., 2005). DNMT1 has a 30-40 fold preference for hemimethylated sites (Cheng and Blumenthal, 2008). DNMT2 appears to contain high sequence and structural similarity; however DNMT2 does not contain any DNA methylating activity. DNMT2 methylates cytosine 38 in the anticodon loop of tRNA (Cheng and Blumenthal, 2008). DNMT2 is also believed to be involved in the recognition of DNA damage, DNA recombination and mutation repair and does not exhibit *de novo* or maintenance activity in either embryonic stem cells, or adult somatic tissues (Turek-Plewa and Jagodzinski, 2005). The DNMT3 family contains two active *de novo* DNMTs. *De novo* is a Latin expression meaning "from the beginning" the DNMT3 family is able to methylate previously unmethylated CpG sites. These *de novo* methyltransferases establish methylation patterns in embryonic stem cells. In the DNMT3 family there are 3 different DNMTs; DNMT3A, DNMT3B, and DNMT3L. DNMT3A and DNMT3B are both active *de novo* DNMTs, DNMT3-Like protein is a regulatory factor (Cheng and Blumenthal, 2008). DNMT3L is known to be involved in maternal genomic imprinting which affects the activity of DNMT3A and 3B, however DNMT3L does not seem to

actively methylate DNA (Cheng and Blumenthal, 2008; Turek-Plewa and Jagodzinski, 2005). Figure 12 displays the different DNMT domains, the conserved catalytic domains lead to activity or lack of activity on DNA.

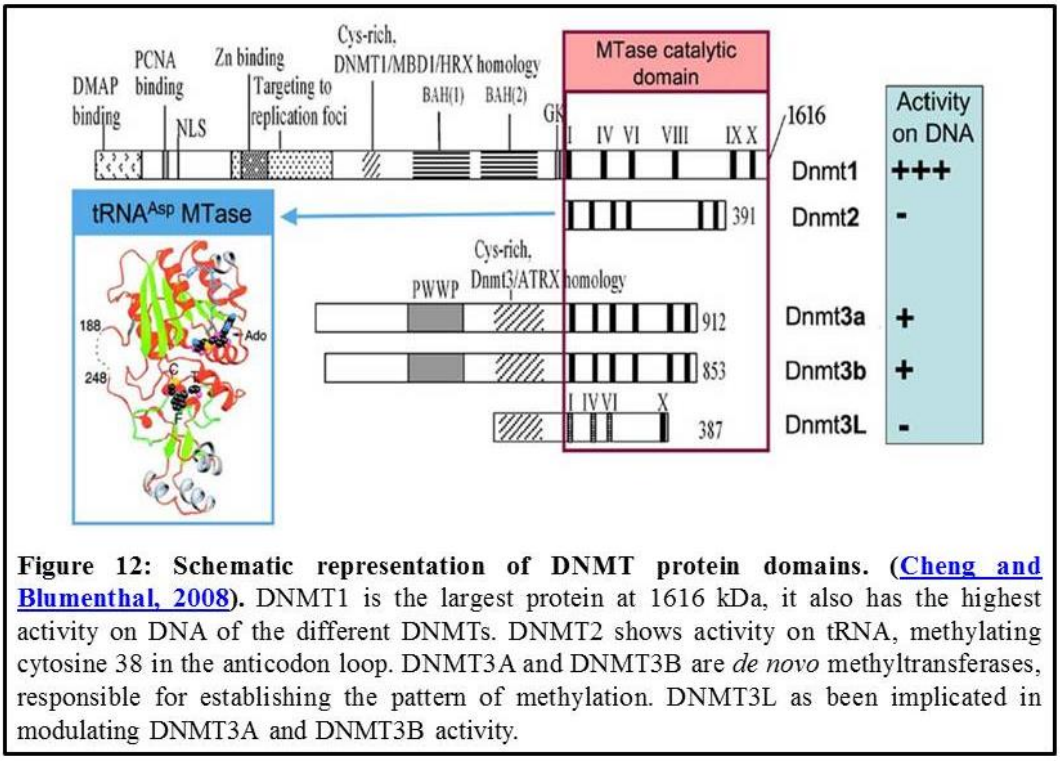

Figure 12: Schematic representation of DNMT protein domains. (Cheng and Blumenthal, 2008). DNMT1 is the largest protein at 1616 kDa, it also has the highest activity on DNA of the different DNMTs. DNMT2 shows activity on tRNA, methylating cytosine 38 in the anticodon loop. DNMT3A and DNMT3B are *de novo* methyltransferases, responsible for establishing the pattern of methylation. DNMT3L as been implicated in modulating DNMT3A and DNMT3B activity.

De novo methylation activity has been shown to be important to embryonic development. DNMT3B knockout mice have multiple developmental defects. These defects include growth impairment and rostral neural tube development. Okano et al. developed DNMT3B knockout mice; none of these mice experienced a live birth. DNMT3A knockout mice also suffered major developmental deficiencies. The DNMT3A mice were able to experience a live birth; however they quickly became runted and died about 4 weeks after birth. DNMT 1 knockout mice were also not viable (Okano et al., 1999).

In addition to playing a key role in the development of cancer, DNA methylation also plays a key role in metabolic regulation in cells. DNA methylation in normal and cancer muscle

cells is altered when exposed to butyrate, a short-chain fatty acid. Similarly, when muscle cells were exposed to acute palmitate, or oleate increased promoter methylation was observed in the mitochondrial protein peroxisome proliferator-activated receptor gamma coactivator 1 α (PGC1α) (Barres et al., 2012). DNA methylation can modify the expression of PGC1α and PPARγ, two transcription factors that are involved in fatty acid storage and glucose metabolism (Barres et al., 2009). This suggests that cellular metabolism is epigenetically regulated by DNA methylation, and may play an important role in cancer metabolism. Cancer cells exhibit an altered basal metabolism. Normal cells produce energy via oxidative phosphorylation occurring in the mitochondria, when starved of oxygen normal cells will produce energy via glycolysis. Cancer cells are less dependent on the mitochondria pathway; instead cancer cells produce a large portion of their ATP via glycolysis regardless of oxygen availability. This phenomenon of altered metabolism was discovered in 1924 by Otto Warburg. Warburg's hypothesis regarding the altered metabolism was that aerobic glycolysis was the primary energy source because mitochondrial (respiratory) injury had occurred (Upadhyay et al., 2013; Warburg, 1956). During glycolysis a large amount of lactic acid builds, creating a highly acidic local environment. Tumor cells proliferate at a high rate in a vastly different environment, tumor cells prefer an acidic environment; they also prefer hypoxic conditions. Micro-environments that lack sufficient oxygen are said to be hypoxic. Hypoxia is associated with tumor progression, metastasis and resistance to therapy (Upadhyay et al., 2013). HIF1α is a critical transcription factor associated with hypoxic conditions, becoming highly upregulated in these conditions. HIF-1 activity has been shown to promote tumor progression, while inhibition of HIF-1 could represent a novel approach to cancer therapy (Semenza, 2002)

Materials and Methods

Cell Culture:

C2C12 mouse myoblasts, HEK293T, and HEK293F human embryonic kidney cells, and human lung adenocarcinoma cells (A549) were cultured under normal conditions prior to treatments with compounds and siRNA. Normal culture conditions includes; Dulbecco's Modified Eagle Medium (DMEM) with the addition of 10% Fetal Bovine Serum (FBS), and 1% penicillin/streptomycin, cells were grown in a 37 °C 5% CO_2 incubator. For differentiation experiments, C2C12 cells were plated at 1.5 x 10^5 cells per well, in a 6-well dish, or 5 x 10^5 cells in a 10 cm plate, DMEM was supplemented with 2% HS, and 1% P/S. Media was changed every other day for 5 days, after which the cells were either lysed, or treated with compounds.

siRNA:

siGENOME SMARTpool- DNMT3B siRNA (M-006395-01-0005), DNMT3A siRNA (M-006672-03-0005), and DNMT1 (M004605-01-0005) were purchased from Dharmacon (Thermo Fisher Scientific Waltham, MA). siGENOME Non-Targeting siRNA Pool #2 served as a control (D-001206-14-05). siNT acts as our control because it is similar to the other siRNA's, however it does not target anywhere in the genome. The siRNA was received lyophilized, and; they were reconstituted in RNase and nuclease-free water at a final concentration of 20 µM, and stored at -80°C per manufacturer's instructions.

siRNA Transfection:

A549 cells were plated on Day 0 at 3 x 10^5 cells per well in a 6-well dish in DMEM supplemented with 10% FBS, without phenol red or antibiotics. The following day, cells were transfected with 100nM siRNA, using DharmaFECT 1, as recommended by the manufacturer.

After 48 hours, culture media were collected and stored at -80°C for future analysis. Cells were incubated for an additional 24 hours before being harvested.

DNMT3A overexpression:

Addgene Plasmid 35521 was received as a stab cultures from Addgene (Cambridge, MA). Vector constructs were produced in the Arthur Riggs laboratory (Chen et al., 2005). Cultures were streaked onto LB agar plates + 100 μg/ml ampicillin (Amp). Single colonies were selected and inoculated in 5 mL of 2X YT media + Amp, and placed in a 37°C shaking incubator for 16 hours at 250 rpm. Plasmid DNA was isolated via Qiagen Plasmid Mini Kit. Plasmids were sequenced by Eurofins US (Huntsville, AL) to confirm the identity of the construct. Large-scale plasmid purification was accomplished with the Zyppy Plasmid Maxi-Prep Kit (Zymo Scientific), (Irvine, CA) and all DNA was brought to a final concentration of 1 mg/ml.

DNMT3B Overexpression:

DNMT3B constructs were generated using Gateway cloning technology. DNMT3B-GFP was generated by performing an LR Clonase reaction (Life Technologies) using pENTR223.1-DNMT3B (Open Biosystems clone 40080753) and pcDNA-DEST47 (Life Technologies) to produce a C-terminal GFP fusion construct driven by the human cytomegalovirus (CMV) promoter. DNMT3B-HIS was generated by performing an LR Clonase reaction (Life Technologies) using pENTR223.1-DNMT3B (Open Biosystems clone 40080753) and pcDNA-DEDT40 (Life Technologies) to produce a C-terminal 6XHIS/V5-fusion construct driven by the CMV promoter. Bother constructs are shown below in Figure 13.

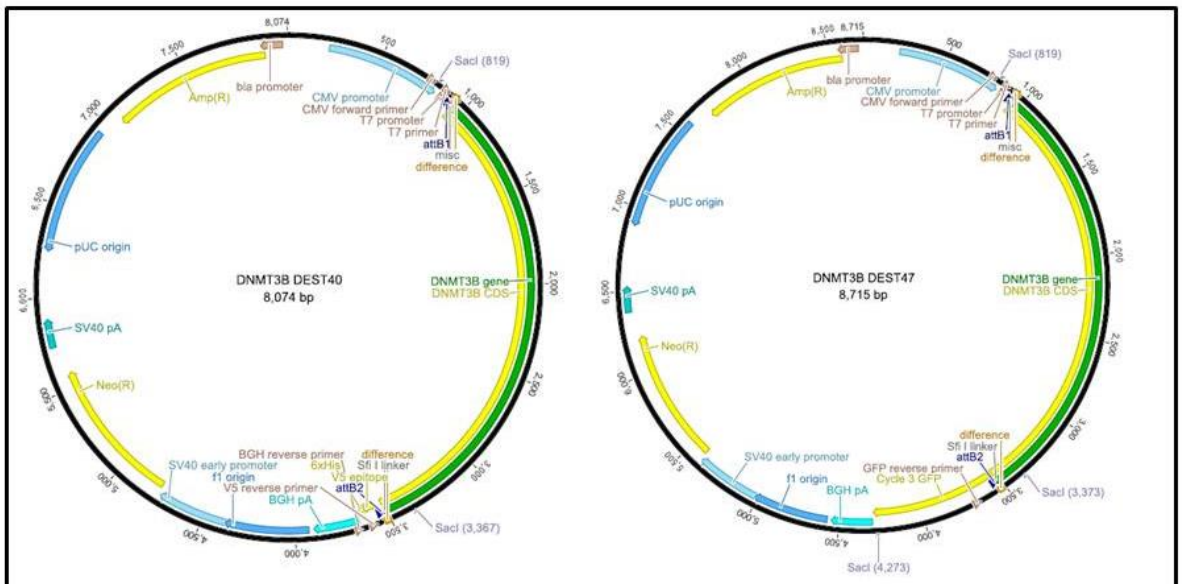

Figure 13: Vector maps of the DNMT3B constructs. We created these constructs using Gateway cloning technology. DNMT3B DEST 40 vector contains A 6x HIS tag fused to the DNMT3B sequence. DNMT3B DEST 47 vector contains GFP fused to the DNMT3B sequence.

Transfection:

A549 cells were plated on Day: 0 at 5*10^5 cells per well in a 6-well dish. 2µg of DNA was incubated in 250µL of Opti-MEM Reduced Serum Media, Lipofectamine 2000 (Life Technologies) was used 3:1 in excess, also incubated in 250µL Opti-MEM. The two components incubated for 5 minutes at room temperature, then incubated together for 20 minutes. 1.5mL of Opti-MEM was added directly onto cells, 500µL of DNA Lipofectamine 2000 was added dropwise to each well. Cells were incubated for 16 hours, then DMEM +10%FBS +1%Pen/Strep was added and incubated for an additional 24 hours.

RNA Collection:

Cells were collected via incubation with Trypsin + EDTA (0.25%) (MediaTech Inc. Manassas, VA) for 4 minutes at 37°C, 5% CO_2, and centrifuged at 1,500 rpm for 3 minutes. Supernatant was removed and cells were snap-frozen on dry ice. Cell pellets were stored at -80°

or processed immediately. Total RNA was extracted using Qiagen's (Valencia, CA) RNeasy Plus Mini Kit according to the manufacturer's instructions.

Reverse Transcriptase PCR:

cDNA was synthesized from 0.5-1 µg of total RNA input using iScript Reverse Transcription Supermix for RT-qPCR Bio-Rad (Hercules, CA. Reactions occurred in a T100 Thermal Cycler (Bio-Rad), following manufacturer's instructions.

Real-Time Quantitative PCR:

Real-Time Quantitative PCR (RT-qPCR) was performed using a Bio-Rad CFX Connect Real-Time PCR Detection System. Data acquisition was performed on Bio-Rad CFX Manager 3.0 software. Each 20 µl reaction was comprised of forward and reverse primers at a final concentration of 500nM, 5 µl cDNA diluted five-fold, 3 µL water, and 10µl SsoAdvanced SYBR Green Supermix (Bio-Rad).

Gene/Target	Primer	%GC	Sequence	Length	T_m	Position
TBP	Left	50	CGGCTGTTTAACTTCGCTTC	20	60	29-48
TBP	Right	50	CACACGCCAAGAAACAGTGA	20	60	87-106
PGC1α	Left	55	CGTGACCACTGACAATGAGG	20	60	468-487
PGC1α	Right	63	GGCTGGTGCCAGTAAGAGC	19	60	558-576
PPARγ	Left	60	TCCGGGCCCTGGCAAAACAT	20	59	879-898
PPARγ	Right	60	TGTCAAGATCGCCCTCGCCT	20	58	942-961
HIF1α	Left	40	TGGAATGGAGCAAAAGACAA	20	59	2696-2715
HIF1α	Right	50	TGGTCAGCTGTGGTAATCCA	20	60	2774-2793
DNMT1	Left	50	CAGCCAACAGAGGACAACAA	20	59	2875-2894
DNMT1	Right	58	TAGAGGACCCGGCTATCCA	19	60	2978-2996
DNMT3A	Left	50	AGACGGCAAATTCTCAGTGG	20	60	543-562
DNMT3A	Right	58	GGGCTGCTTGTTGTACGTG	19	60	618-636
DNMT3A	Left	60	GCCAGGCCGCATTGTGTCTT	20	58.2	469-488
DNMT3A	Right	57	AGCTCAGCGGCATCAGCTTCT	21	58.6	576-596
DNMT3B	Left	50	ATAAGTCGAAGGTGCGTCGT	20	53.8	1394-1413
DNMT3B	Right	45	GGCAACATCTGAAGCCATTT	20	51.2	1577-1596

Table 2: List of Primers used for qRT-PCR analysis.

Protein Collection and Concentration Assay:

Cells were collected using trypsin, centrifuged for 3 minutes at 1,500 rpm at 4°C. Cells were then lysed in 1X RIPA buffer containing 1X PhosSTOP (Roche Kaiseraugst, Switzerland), and 1X Protease Inhibitor(Roche). Depending on the plate size the volume of RIPA buffer was adjusted accordingly. Samples were subjected to 30 second sonication, and then centrifuged at 15,000 x *g* for 30-40 minutes at 4°C. A Bradford-Coomassie Assay (Pierce/ Thermo Fisher Scientific) was performed to determine the concentration of total protein per sample.

Western Blot Analysis:

50-150μg of protein per sample was run on Invitrogen's NuPAGE SDS-PAGE Gel System using 1.0 mm 4-12% Bis-Tris precast gels in 1X MOPS running buffer following the manufacturer's instructions. Transfers were done following manufacturer's instructions and membranes were blocked for one hour at room temperature with 5% milk in 1XTBST. PhosSTOP phosphate inhibitor cocktail(Roche) was added to the blocking buffer for membranes that were to be probed with specific antibodies.

Antibodies:

Primary antibodies were purchased from Cell Signaling Technology (Boston, MA) unless otherwise stated. They were used as instructed by manufacturer. Mouse anti DNMT3A antibody was purchased from New England BioLabs Inc. (Ipswich, MA), used at a final concentration of 1:1,000. Antibodies were diluted in 5% non-fat dry milk in 1XTBST. 5% Sodium Azide (NaN_3) was added at a 1:100 dilution, To serve as a preservative. Secondary antibodies were purchased from Cell Signaling Technology and GE Healthcare (Waukesha, WI), and diluted at 1:2,000 in 5% non-fat milk in 1XTBST.

Immunoprecipitation:

Pierce A/G Magnetic beads were a generous gift by the Lunyak Lab. 500µl of sample was combined with 5 µl of 1° antibody and incubated overnight at 4°C. Beads were washed, and then incubated with sample for 5 hours. Samples were then heated for 10 minutes at 100°C. 20µl of sample was then run on a 4-12% Bis-Tris precast gels in 1X MOPS running buffer per manufacturers instructions.

Results and Discussion

DNMT3B Endogenous Protein Immunoprecipitation:

We began examining the *de novo* methyltransferase DNMT3B with great interest. The two active *de novo* DNMT's are of great interest because they are responsible for establishing the pattern of methylation. This causes gene silencing, which is fundamental in cancer development. However, methylation is not only important in cancer development. DNA methylation also has also been shown to play a role in cellular metabolism and physiology. Isolation of the protein would allow us to examine the crystal structure using mass spectrometry. We first wanted to examine the DNMT3B protein to measure endogenous levels. We started by conducting a western blot. Lane 2 and lane 3 are both control samples. DNMT3B has a molecular weight of 96 kDa.

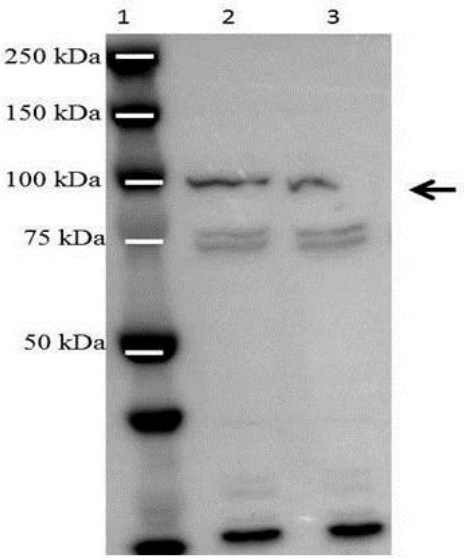

Figure 14: Western blot of DNMT3B levels in HEK293T whole cell lysate: Lane 1- Precision Plus2 Prestained Protein Ladder (Bio-Rad) Lane 2- Ctrl 293T whole cell lysate, Lane 3- Ctrl 293T whole cell lysate. Approximately 180µg of protein were loaded per well. The arrow indicates ~96 kDa the approximate location of the DNMT3B protein.

The total amount of protein that was loaded into each well was approximately 180µg of protein and the DNMT3B protein showed a very slight band pattern. After determining low expression via western blot as shown in Figure 14, an immunoprecipitation was conducted. The goal of immunoprecipitating the protein was to excise the band from the gel, and examine the crystal structure of the band using mass spectrometry.

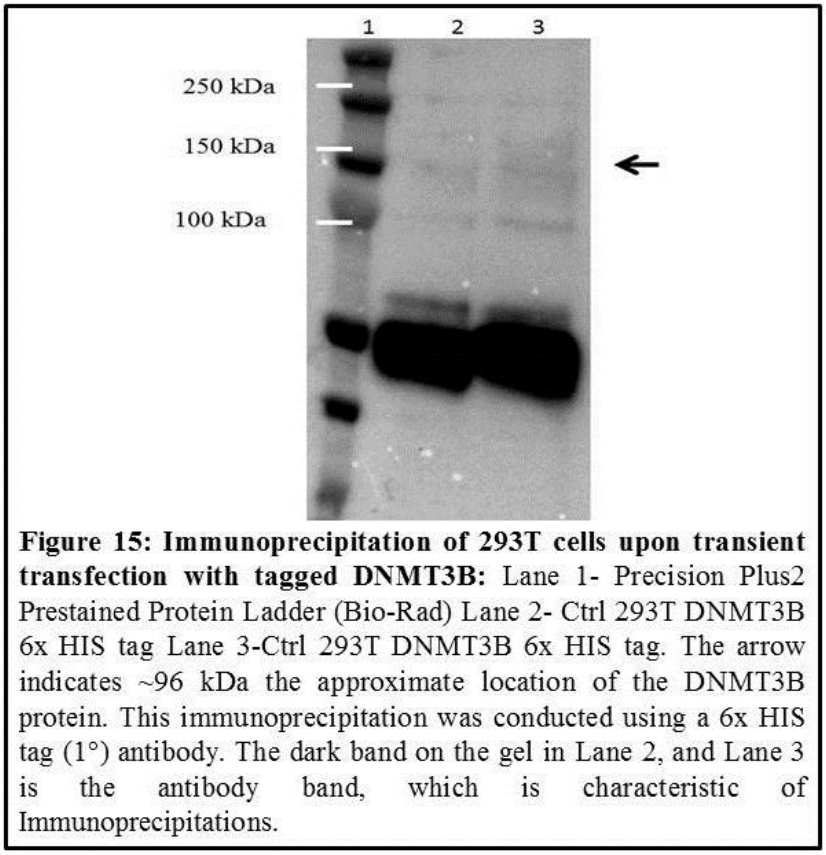

Figure 15: Immunoprecipitation of 293T cells upon transient transfection with tagged DNMT3B: Lane 1- Precision Plus2 Prestained Protein Ladder (Bio-Rad) Lane 2- Ctrl 293T DNMT3B 6x HIS tag Lane 3-Ctrl 293T DNMT3B 6x HIS tag. The arrow indicates ~96 kDa the approximate location of the DNMT3B protein. This immunoprecipitation was conducted using a 6x HIS tag (1°) antibody. The dark band on the gel in Lane 2, and Lane 3 is the antibody band, which is characteristic of Immunoprecipitations.

After multiple trials of trying to immunoprecipitate the protein we were unable to see the DNMT3B protein band. Two vector constructs were used in our attempt to immunoprecipitate the protein. A DEST40 vector containing the DNMT3B protein fused to a 6x HIS tag, and a DEST 47 vector containing the DNMT3B protein fused to GFP. The GFP was used as a transfection control to ensure transfection efficiency. Unfortunately, 48 hours post transfection a very small amount of GFP was present in the DEST 47 transfected cells. (data not shown)

DNMT3B Overexpression Western Blot:

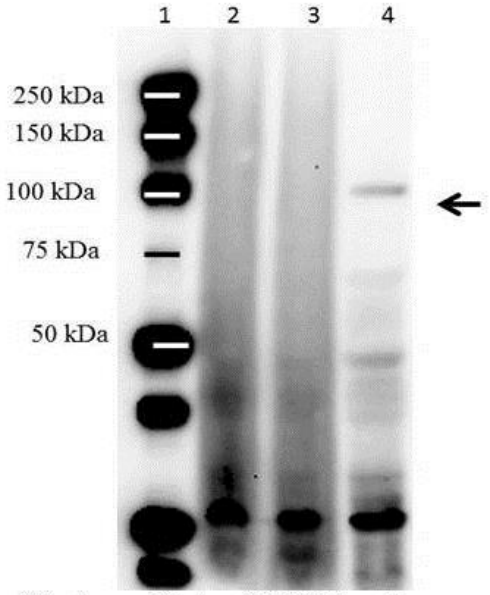

Figure 16: Western Blot of 293F cells upon transient transfection with tagged DNMT3B: Lane 1- Precision Plus2 Prestained Protein Ladder (Bio-Rad) Lane 2- Ctrl 293T DNMT3B 6x HIS tag, Lane 3-Ctrl 293T DNMT3B 6x HIS tag, Lane 3-Ctrl 293T DNMT3B 6x HIS tag. The arrow indicates ~96 kDa the approximate location of the DNMT3B protein. This western blot was conducted using a 6x HIS tag (1°) antibody.

When we did not see the protein bands via immunoprecipitation we decided to ensure the band could be seen once conducting a transient transfection and preforming a western blot. Figure 16 shows that we were only able to detect a protein band in one lane, and at very minute amounts. The results obtained from all western blot analyses, and immunoprecipitations prompted moving from a normal cell, to a cancer cell.

DNMT3B Endogenous Protein Expression in A549 Adenocarcinoma Cells

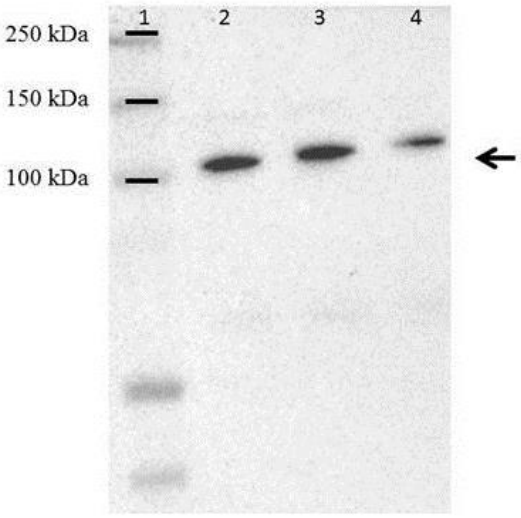

Figure 17: Western Blot analysis of A549 cells probed with DNMT3B antibody: Lane 1- Precision Plus2 Prestained Protein Ladder (Bio-Rad) Lane 2- Ctrl A549 whole cell lysate, Lane 3-Ctrl A549 Whole cell lysate, Lane 4-Ctrl A549 whole cell lysates. The arrow indicates ~96 kDa the approximate location of the DNMT3B protein. This western blot was conducted using a DNMT3B (1°) antibody.

A549 lung adenocarcinoma cells are known to have higher expression levels of DNMT3B. Western blot analysis confirmed, Figure 17 shows A549 cells grown in a 10-cm dish, cells were collected and prepared. Each lane was loaded with 44µg of protein. Purifying the DNMT3B protein proved more difficult than initially anticipated, therefore we decided to examine an alternative method of protein manipulation. Overexpression of the DNMT3B protein is still of great interest. Further optimizations of overexpression protocols are necessary.

siRNA Mediated Silencing of DNMT1, DNMT3A, DNMT3B

Using RNA interference (RNAi) to silence DNMT1, DNMT3A, and DNMT3B genes allows us to study the effects of these genes, and their importance. To test the level of

knockdown in samples qRT-PCR analysis was completed, the level of knockdown was ascertained. As seen in Figure 18 knockdown efficiencies were successful, approximately 80%.

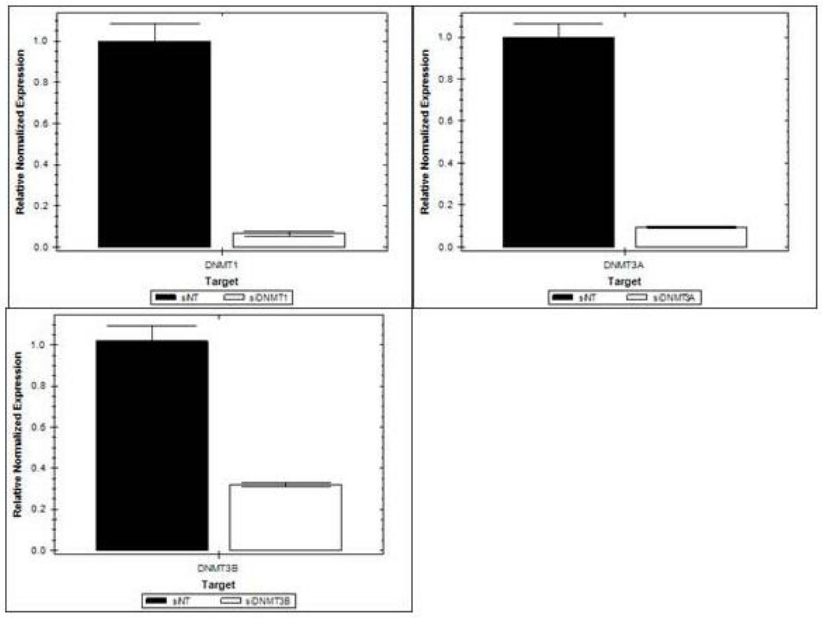

Figure 18: siRNA mediated knockdown of DNMTs in A549 cells. All samples were treated with siRNA for 72 hours, then mRNA levels were measured via qRT-PCR. Knockdown efficiency is listed in Table 3 (below).

DNMT	Level of knockdown (%)
DNMT1	93%
DNMT3A	90%
DNMT3B	68%

Table 3: % knockdown post siRNA mediated gene silencing

A549 Show Increased Sensitivity to Glycolytic and Mitochondrial Inhibitors when DNMT's are Knocked Down

Once the level of gene knockdown was confirmed, glycolytic and mitochondrial inhibitors were tested to examine the role DNMTs play in regulating cellular metabolism, specifically lung cancer metabolism. Cancer cell metabolism differs from non-meiotic cells in ATP production. Cancer cells and other highly proliferative tissues acquire a large portion of their energy from glycolysis, whereas non-meiotic cells produce large amounts of ATP via oxidative phosphorylation in the mitochondria. This prompted examination of multiple metabolic inhibitors. A549 cells were transiently transfected with 100nM siRNA for 48 hours, siRNA was then removed and inhibitors were added. Figure 11 shows the effects of the different glycolytic and mitochondrial inhibitors on ATP production levels. A CellTiter-Glo Assay (Promega Madison, WI) measures ATP, which is representative of metabolically active cells. Normal glucose containing media was used as a control for all samples. Galactose forces cells into mitochondrial respiration because oxidation of galactose to pyruvate via glycolysis yields no net ATP. (Marroquin et al., 2007). The next inhibitor used was 2-deoxyglucose, which is a glucose analogue that competitively inhibits hexokinase activity in the first enzymatic step of glycolysis. (Suchorolski et al., 2013) Bromo-pyruvate is also a hexokinase II inhibitor.(Nakano et al., 2011) Oligomycin was the next inhibitor; oligomycin inhibits the mitochondrial ATP synthase. (Zhang et al., 2012b) The final inhibitor used was rotenone, rotenone is a potent mitochondrial complex I inhibitor. (Xiong et al., 2013) In figure 11 A549 cells were treated with siRNA for 48 hours, then the media was changed and compounds were added. Upon addition of compounds all siRNA mediated knockdown samples showed increased sensitivity towards glycolytic and mitochondrial inhibitors.

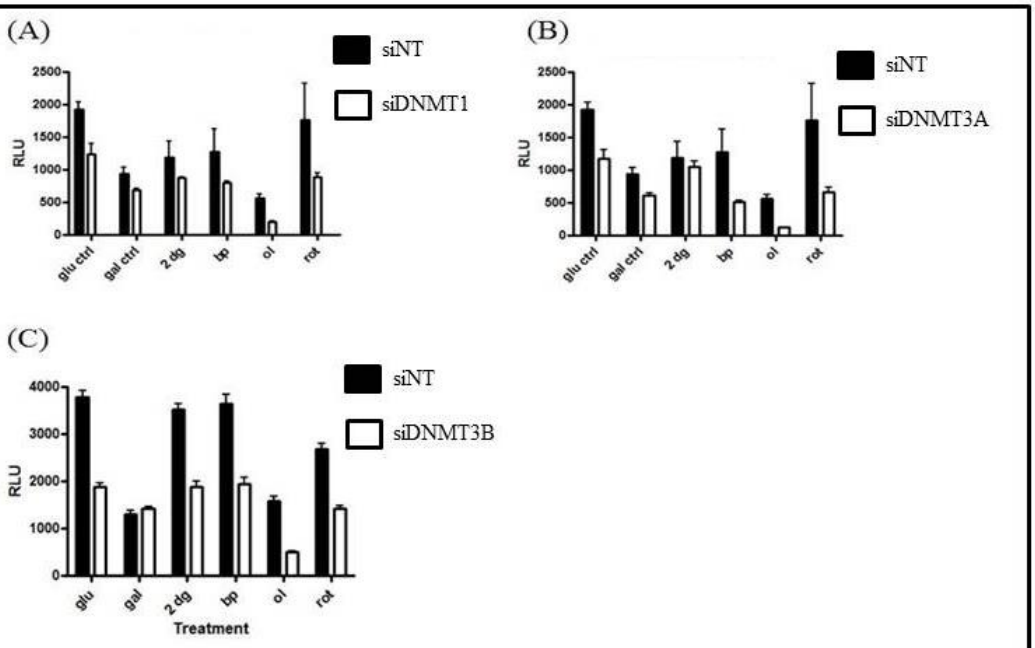

Figure 19: siRNA mediated knockdown, followed by the treatment with glycolytic and mitochondrial inhibitors. (A)-DNMT1 shows increased sensitivity towards both glycolytic and mitochondrial inhibitors. (B) DNMT3A shows an increase in sensitivity towards glycolytic, and a dramatic increase towards mitochondrial inhibitors. (C)-DNMT3B also showed an increase in sensitivity towards the inhibitors, however when grown in galactose the DNMT3B knockdown samples showed increased viability.

The altered basal metabolism cancer cells experience has been known for about 100 years. Otto Warburg's hypothesis regarding cancer cells preference towards glycolysis is still a mystery. Figure 19 shows A549 cells treated with siRNA, and then treated with compounds that inhibit the glycolytic (2-DG, BP) or mitochondrial pathway (OL, ROT) cellular viability is decreased dramatically. DNMT1 knock-down shows increased sensitivity, but cells are not quite as inhibited by glycolytic inhibitors as DNMT3B knockdown samples. DNMT3B shows a dramatic loss in viability when treated with glycolytic inhibitors, which shows DNMT3B could be mediating glycolysis. Whether the effect is causal, or cooperative is unknown. DNMT3A shows a similar trend towards sensitivity when treated with inhibitors, however the effect is less dramatic when treated with 2-DG. Interestingly 2-DG and BP had differing results. 2-DG showed a slight increase in sensitivity, where BP showed a very extreme sensitization.

Oligomycin is a potent inhibitor of ATP synthase. Not surprisingly, oligomycin showed a very dramatic effect in all the DNMT knockdown samples. Rotenone also displayed a similar effect. Due to the large amount of sensitivity conveyed by the different inhibitors, we believe DNMT's are important for metabolism.

Global Analysis of Metabolites after DNMT Knockdown via HPLC-MS

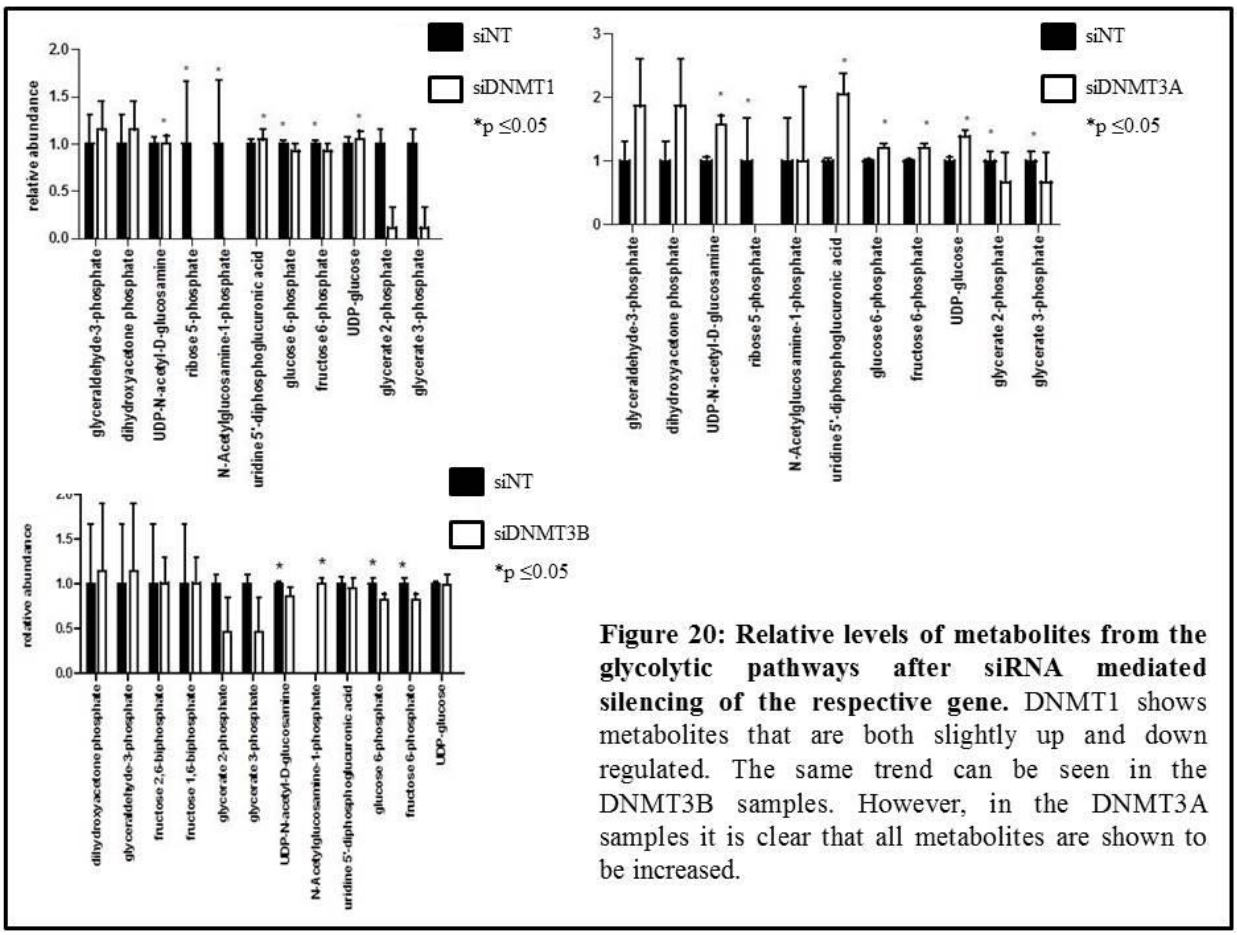

Figure 20: Relative levels of metabolites from the glycolytic pathways after siRNA mediated silencing of the respective gene. DNMT1 shows metabolites that are both slightly up and down regulated. The same trend can be seen in the DNMT3B samples. However, in the DNMT3A samples it is clear that all metabolites are shown to be increased.

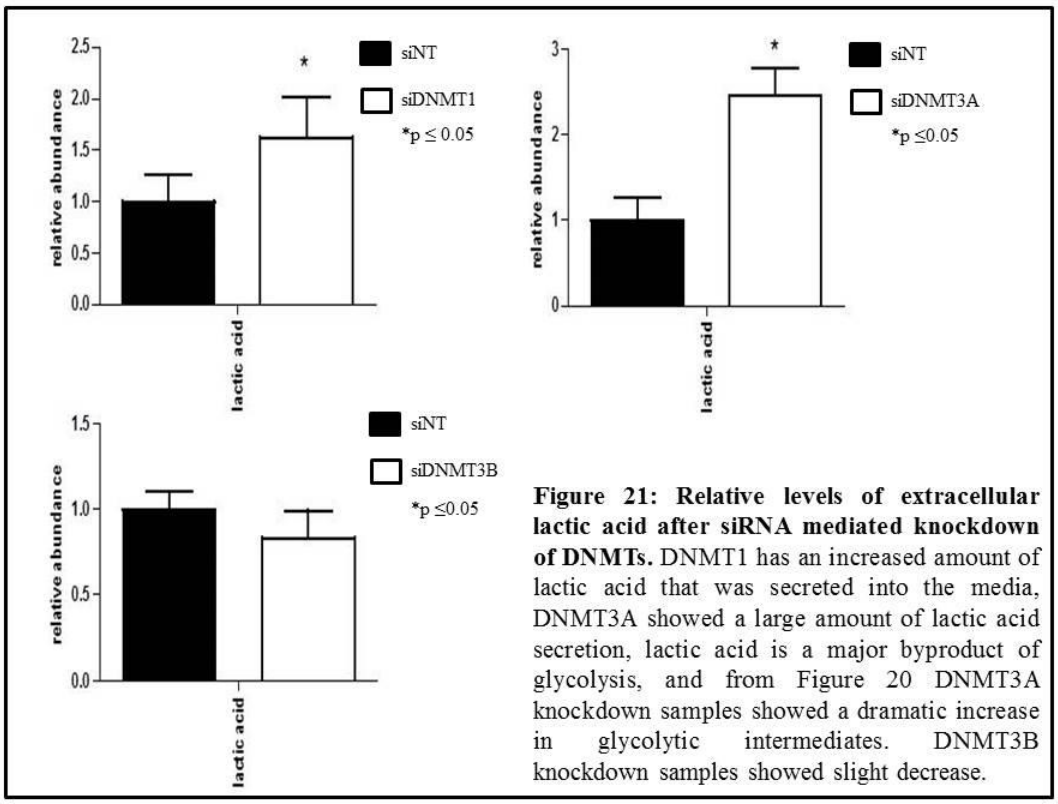

Figure 21: Relative levels of extracellular lactic acid after siRNA mediated knockdown of DNMTs. DNMT1 has an increased amount of lactic acid that was secreted into the media, DNMT3A showed a large amount of lactic acid secretion, lactic acid is a major byproduct of glycolysis, and from Figure 20 DNMT3A knockdown samples showed a dramatic increase in glycolytic intermediates. DNMT3B knockdown samples showed slight decrease.

Figure 20 represents metabolites from the glycolytic pathway. DNMT1 knockdown samples show a slightly reduced level of glycolytic intermediates, the changes seen are slight, however they are statistically significant. The amount of lactic acid produced by DNMT1 knockdown is much higher than control samples. The DNMT3A knockdown samples show an increase in a large portion of glycolytic intermediates, silencing of the DNMT3A gene shows an upregulation in glycolysis. This is also confirmed by figure 21 showing a large increase in lactic acid present. Glycolysis is a rapid way of producing ATP, a byproduct is lactic acid. Following a similar trend as the DNMT1 knockdown, DNMT3B shows significantly altered metabolites, both up and down regulated. The extracellular fingerprinting of lactic acid on DNMT3B media confirms that lactic acid production is slightly less than control samples. The most dramatic difference in glycolysis was seen in the DNMT3A knockdown samples.

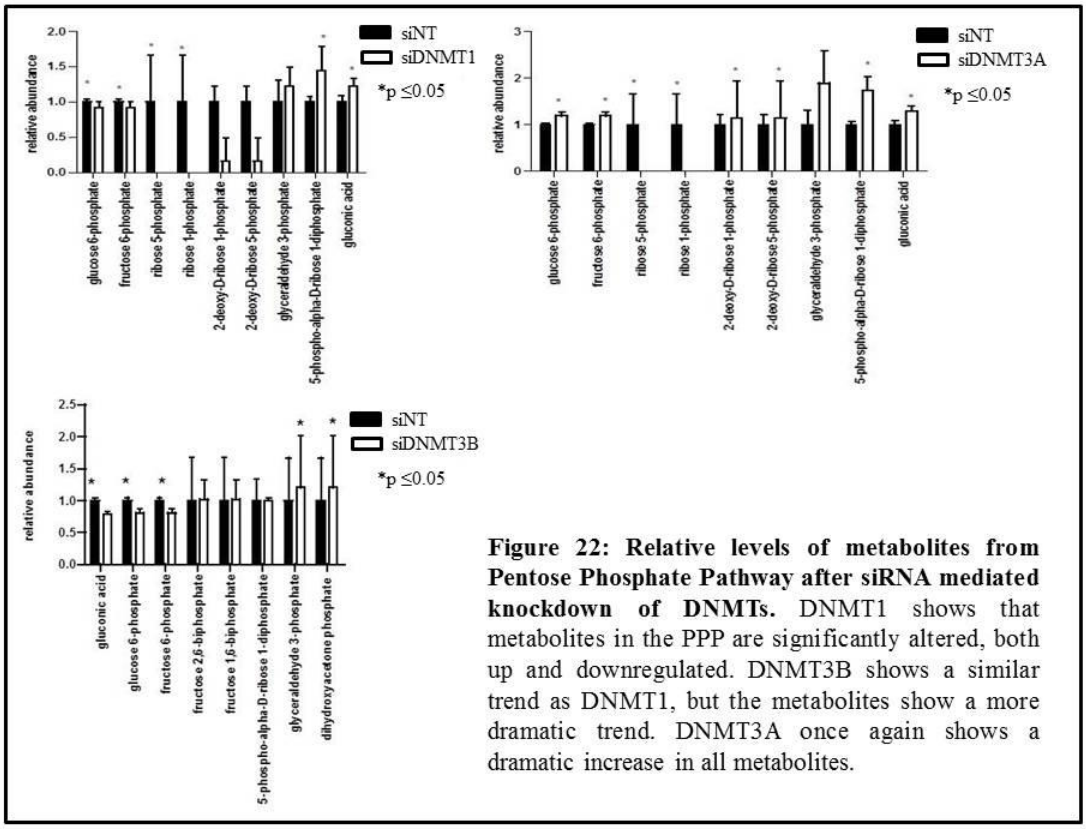

Figure 22: Relative levels of metabolites from Pentose Phosphate Pathway after siRNA mediated knockdown of DNMTs. DNMT1 shows that metabolites in the PPP are significantly altered, both up and downregulated. DNMT3B shows a similar trend as DNMT1, but the metabolites show a more dramatic trend. DNMT3A once again shows a dramatic increase in all metabolites.

The pentose phosphate pathway (PPP) is important for two main reasons, one is the production of ribose-5-phosphate (R5P), which is used for the synthesis of nucleotides, and also the formation of NADPH which protects against oxidative stress. NADPH neutralizes reactive oxygen intermediates. (Perl et al., 2011) In figure 22 we can see that DNMT1, and DNMT3B have similar patterns of metabolites, this was also seen in the glycolytic pathway. Metabolites from the pathway are significantly up and down regulated. These data points suggest that DNMT1 and DNMT3B enzymes have similar characteristics in metabolism. DNMT3A shows a different pattern. DNMT3A shows a very strong trend towards upregulation of metabolites and intermediate products.

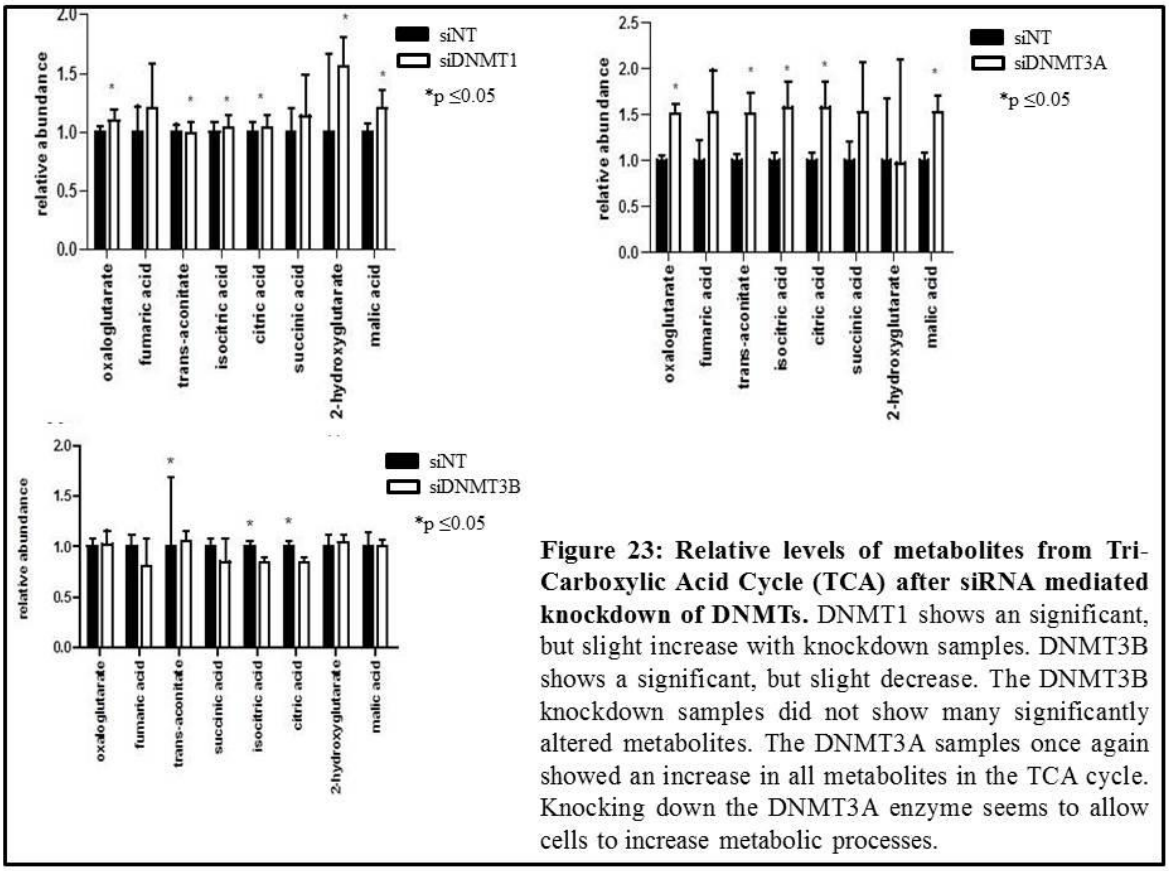

Figure 23: Relative levels of metabolites from Tri-Carboxylic Acid Cycle (TCA) after siRNA mediated knockdown of DNMTs. DNMT1 shows an significant, but slight increase with knockdown samples. DNMT3B shows a significant, but slight decrease. The DNMT3B knockdown samples did not show many significantly altered metabolites. The DNMT3A samples once again showed an increase in all metabolites in the TCA cycle. Knocking down the DNMT3A enzyme seems to allow cells to increase metabolic processes.

Figure 23 represents metabolites in the tricarboxylic acid (TCA) cycle, also known as Krebs cycle. The TCA cycle is the major final common pathway for oxidation of carbohydrates, lipids, and some amino acids, resulting in large amounts of ATP via oxidative phosphorylation. Fluctuation of the TCA cycle directly affects oxidative phosphorylation. (Bowtell et al., 2007) Figure 23 shows intermediate metabolites of the TCA cycle. In this pathway all DNMT's seem to have a slightly different affect. The DNMT1 knockdown samples are all slightly increased, the most dramatic increase being 2-hydroxygluterate, and malic acid. DNMT3A knockdown samples a very noticeably increased in all metabolites and intermediate products. DNMT3B shows a small amount of decrease in some metabolites, of all the conditions DNMT3B seems to have to smallest effect in the TCA cycle.

Figures: 20, 21, 22, 23 show global metabolite changes after treatment with siRNA. The amount of metabolites and intermediates that are both increased and decreased show that all DNMT's play a role in cellular metabolism. DNMT3A knockdown seems to have the most significant effect in all pathways. DNMT3A knockdown samples seem to increase all metabolites in glycolysis, PPP, and TCA cycle. These three cycles differ in many respects, which lead us to believe that DNMT3A is very significantly involved in cellular metabolism. Analysis of these pathways and transcription factors that could be involved in the metabolism changes prompts investigation into energy signaling.

Transcription Factors Involved in DNMT Mediated Metabolism:

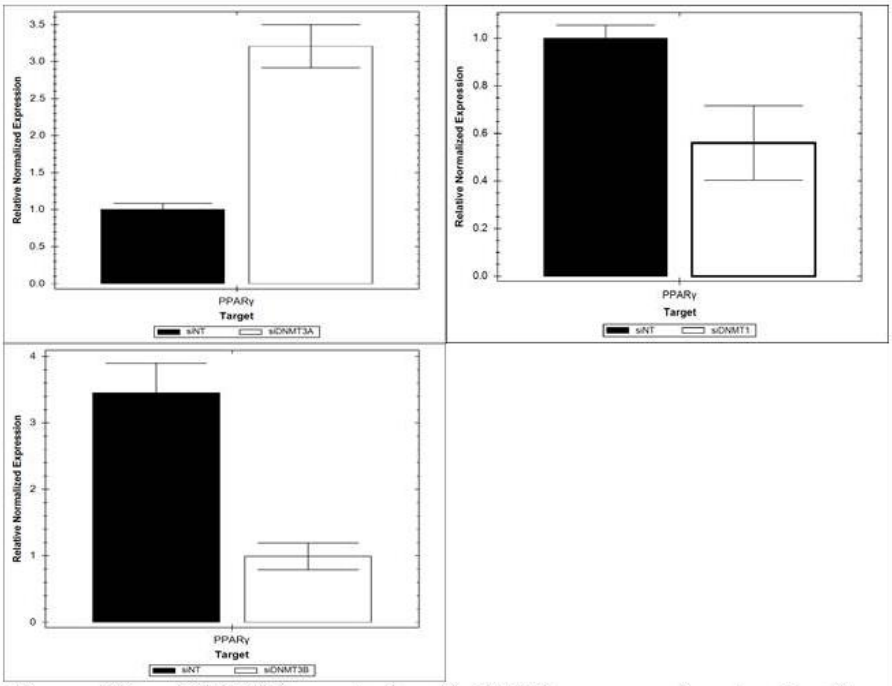

Figure 24: qRT-PCR analysis of PPARγ expression level after DNMT1, DNMT3A, and DNMT3B siRNA mediated silencing. PPARγ expression does not change with DNMT1 gene silencing. DNMT3A causes a 2 fold increase in PPARγ expression. DNMT3B shows a different affect, with a large decrease in expression upon gene silencing.

PPARγ is a member of the nuclear hormone receptor suerfamily. PPARγ is associated with sensing fatty acids, and other nutritional signals (Semple et al., 2006). DNMT1 silencing does not seem to alter the expression level of PPARγ, however DNMT3A, and DNMT3B seem to have differential effects on PPARγ expression levels. DNMT3A causes a 2-fold increase, where DNMT3B causes almost a 1.5 fold decrease in expression level.

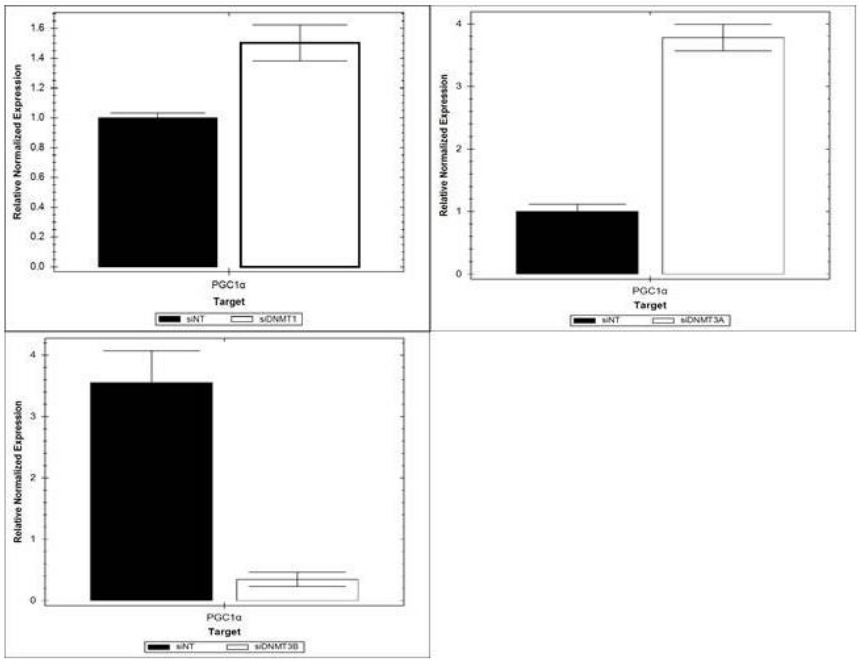

Figure 25: qRT-PCR analysis of PGC1α expression level after DNMT1, DNMT3A, and DNMT3B siRNA mediated silencing. Both DNMT1 and DNMT3A showed an increase in PGC1α expression upon gene silencing, on the other hand DNMT3B showed a dramatic expression decrease upon gene silencing.

PGC1α is a key transcriptional regulator of lipogenesis and oxidative metabolism. PGC1α has been implicated in cancer development, however different sources have reported opposing results. Initially lower PGC1α expression was associated with cancerous tissue. Conversely, PGC1α expression has been shown in cancer cell proliferation. (Bhalla et al., 2011) Figure X represents the expression level of PGC1α. Both DNMT1, and DNMT3A knockdown samples show elevated PGC1α levels. In contrast DNMT3B samples show a large decrease in expression.

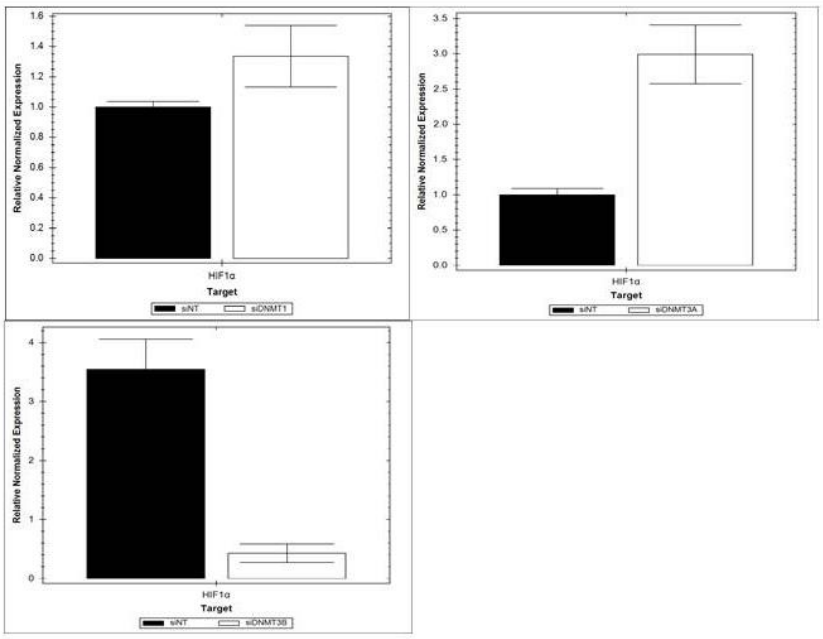

Figure 26: qRT-PCR analysis of HIF-1α expression level after DNMT1, DNMT3A, and DNMT3B siRNA mediated silencing DNMT1 showed a slight increase in HIF1α expression upon gene silencing. DNMT3A also showed an increase in HIF1α expression, however the increase was far more dramatic than DNMT1 samples. DNMT3B showed a slight decrease.

Hypoxic-Inducible factor 1α (HIF-1α) is a transcription factor that mediates adaptive responses to reduced O_2 availability, including angiogenesis and glycolysis. Expression of HIF-1α increases dramatically when cells are hypoxic. DNMT1, and DNMT3B knockdown does not seem to alter the level of HIF-1α, DNMT3A knockdown seems to have a large effect on HIF-1α expression.

Conclusions:

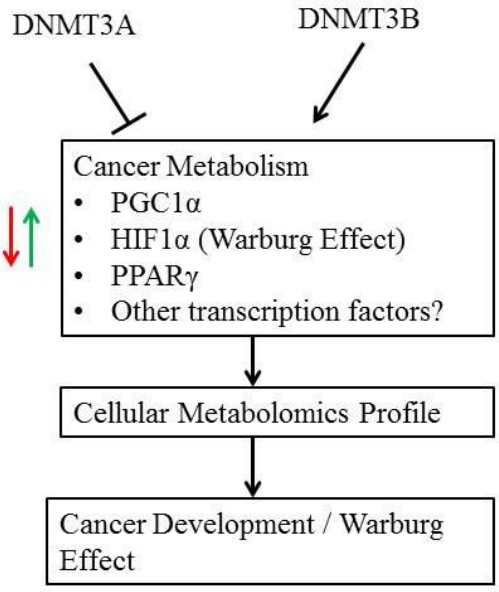

Figure 27: *de novo* DNA methyltransferases 3A and 3B control of cancer metabolism via metabolic transcription factors. Based on preliminary evidence we hypothesized that cancer metabolism is epigenetically regulated by *de novo* DNMTs. A possible mechanism for this is via the a DNMT mediated transcriptional regulation of transcription factors (T.F.) involved in metabolism. PGC1α is a transcription factor, which is a master regulator of mitochondrial biogenesis, and energy homeostasis. PPARγ regulates fatty acid storage and glucose metabolism. HIF1α is important in oxygen homeostasis and becomes highly upregulated during oxygen deprivation, which is a known aspect of the Warburg Effect. Understanding the DNA methylation mediated regulation of these metabolic transcription factors could shed light on the epigenetic basis of the Warburg Effect.

Figures 24, 25, 26 show expression level of samples; promoter methylation status is not taken into account. Promoter methylation analysis is the next step. The data collected thus far shows that DNMT1 is important in metabolism and silencing the gene causes global metabolism changes. DNMT3B is also important in metabolism. DNMT3B is also important in regulating transcription factors associated with metabolic homeostasis. DNMT3A seems to have the most dramatic effect in metabolism. DNMT3A knockdown samples showed a more ideal environment for cancer cell proliferation. The lactic acid increase, increased sensitivity to both glycolytic and mitochondrial inhibitors, and the high induction of HIF1α all suggest that DNMT3A is playing a significant role in cancer metabolism. As previously mentioned promoter methylation status is the next step in determining what genes are being expressed. Enzymatic activity assay kits that measure DNMT activity are also available. Determining DNMTs exact mechanism in the context of cancer cell metabolism will ideally shed light on the Warburg Effect.

References:

Administration, O.S.a.H. Occupational Safety and Health Guideline for Chloroform (United States Department of Labor).

Alder, L., Greulich, K., Kempe, G., and Vieth, B. (2006). Residue analysis of 500 high priority pesticides: better by GC-MS or LC-MS/MS? Mass spectrometry reviews *25*, 838-865.

Allen, J., Davey, H.M., Broadhurst, D., Heald, J.K., Rowland, J.J., Oliver, S.G., and Kell, D.B. (2003). High-throughput classification of yeast mutants for functional genomics using metabolic footprinting. Nature biotechnology *21*, 692-696.

Barres, R., Osler, M.E., Yan, J., Rune, A., Fritz, T., Caidahl, K., Krook, A., and Zierath, J.R. (2009). Non-CpG methylation of the PGC-1alpha promoter through DNMT3B controls mitochondrial density. Cell metabolism *10*, 189-198.

Barres, R., Yan, J., Egan, B., Treebak, J.T., Rasmussen, M., Fritz, T., Caidahl, K., Krook, A., O'Gorman, D.J., and Zierath, J.R. (2012). Acute exercise remodels promoter methylation in human skeletal muscle. Cell metabolism *15*, 405-411.

Bhalla, K., Hwang, B.J., Dewi, R.E., Ou, L., Twaddel, W., Fang, H.B., Vafai, S.B., Vazquez, F., Puigserver, P., Boros, L., *et al.* (2011). PGC1alpha promotes tumor growth by inducing gene expression programs supporting lipogenesis. Cancer research *71*, 6888-6898.

Bowtell, J.L., Marwood, S., Bruce, M., Constantin-Teodosiu, D., and Greenhaff, P.L. (2007). Tricarboxylic acid cycle intermediate pool size: functional importance for oxidative metabolism in exercising human skeletal muscle. Sports Med *37*, 1071-1088.

Buszewski, B., and Noga, S. (2012). Hydrophilic interaction liquid chromatography (HILIC)--a powerful separation technique. Analytical and bioanalytical chemistry *402*, 231-247.

Chen, Z.X., Mann, J.R., Hsieh, C.L., Riggs, A.D., and Chedin, F. (2005). Physical and functional interactions between the human DNMT3L protein and members of the de novo methyltransferase family. Journal of cellular biochemistry *95*, 902-917.

Cheng, X., and Blumenthal, R.M. (2008). Mammalian DNA methyltransferases: a structural perspective. Structure *16*, 341-350.

Denison, M.S., Pandini, A., Nagy, S.R., Baldwin, E.P., and Bonati, L. (2002). Ligand binding and activation of the Ah receptor. Chemico-biological interactions *141*, 3-24.

Dettmer, K., Aronov, P.A., and Hammock, B.D. (2007). Mass spectrometry-based metabolomics. Mass spectrometry reviews *26*, 51-78.

Frooninckx, L., Van Rompay, L., Temmerman, L., Van Sinay, E., Beets, I., Janssen, T., Husson, S.J., and Schoofs, L. (2012). Neuropeptide GPCRs in C. elegans. Frontiers in endocrinology *3*, 167.

Fukushige, S., and Horii, A. (2013). DNA methylation in cancer: a gene silencing mechanism and the clinical potential of its biomarkers. The Tohoku journal of experimental medicine *229*, 173-185.

Gosetti, F., Mazzucco, E., Zampieri, D., and Gennaro, M.C. (2010). Signal suppression/enhancement in high-performance liquid chromatography tandem mass spectrometry. Journal of chromatography A *1217*, 3929-3937.

Greco, G., and Letzel, T. (2013). Main Interactions and Influences of the Chromatographic Parameters in HILIC Separations. Journal of chromatographic science.
Heiger, D. (2000). An Introduction High Performance Capillary Electrophroesis (Germany: Agilent Technologies).
Jones, P.A., and Baylin, S.B. (2002). The fundamental role of epigenetic events in cancer. Nature reviews Genetics *3*, 415-428.
Kleckner, I.R., and Foster, M.P. (2011). An introduction to NMR-based approaches for measuring protein dynamics. Biochimica et biophysica acta *1814*, 942-968.
Lei, Z., Huhman, D.V., and Sumner, L.W. (2011). Mass spectrometry strategies in metabolomics. The Journal of biological chemistry *286*, 25435-25442.
Liu, H., Zhou, Y., Boggs, S.E., Belinsky, S.A., and Liu, J. (2007). Cigarette smoke induces demethylation of prometastatic oncogene synuclein-gamma in lung cancer cells by downregulation of DNMT3B. Oncogene *26*, 5900-5910.
Ma, Y., Zhang, P., Yang, Y., Wang, F., and Qin, H. (2012). Metabolomics in the fields of oncology: a review of recent research. Molecular biology reports.
Marroquin, L.D., Hynes, J., Dykens, J.A., Jamieson, J.D., and Will, Y. (2007). Circumventing the Crabtree effect: replacing media glucose with galactose increases susceptibility of HepG2 cells to mitochondrial toxicants. Toxicological sciences : an official journal of the Society of Toxicology *97*, 539-547.
Metzger, J., Schanstra, J.P., and Mischak, H. (2009). Capillary electrophoresis-mass spectrometry in urinary proteome analysis: current applications and future developments. Analytical and bioanalytical chemistry *393*, 1431-1442.
Mortusewicz, O., Schermelleh, L., Walter, J., Cardoso, M.C., and Leonhardt, H. (2005). Recruitment of DNA methyltransferase I to DNA repair sites. Proceedings of the National Academy of Sciences of the United States of America *102*, 8905-8909.
Nakano, A., Tsuji, D., Miki, H., Cui, Q., El Sayed, S.M., Ikegame, A., Oda, A., Amou, H., Nakamura, S., Harada, T., *et al.* (2011). Glycolysis inhibition inactivates ABC transporters to restore drug sensitivity in malignant cells. PloS one *6*, e27222.
Nebert, D.W., Roe, A.L., Dieter, M.Z., Solis, W.A., Yang, Y., and Dalton, T.P. (2000). Role of the aromatic hydrocarbon receptor and [Ah] gene battery in the oxidative stress response, cell cycle control, and apoptosis. Biochemical pharmacology *59*, 65-85.
Newgard, C.B., An, J., Bain, J.R., Muehlbauer, M.J., Stevens, R.D., Lien, L.F., Haqq, A.M., Shah, S.H., Arlotto, M., Slentz, C.A., *et al.* (2009). A branched-chain amino acid-related metabolic signature that differentiates obese and lean humans and contributes to insulin resistance. Cell metabolism *9*, 311-326.
Nguyen, L.P., and Bradfield, C.A. (2008). The search for endogenous activators of the aryl hydrocarbon receptor. Chemical research in toxicology *21*, 102-116.
Okano, M., Bell, D.W., Haber, D.A., and Li, E. (1999). DNA methyltransferases Dnmt3a and Dnmt3b are essential for de novo methylation and mammalian development. Cell *99*, 247-257.

Perl, A., Hanczko, R., Telarico, T., Oaks, Z., and Landas, S. (2011). Oxidative stress, inflammation and carcinogenesis are controlled through the pentose phosphate pathway by transaldolase. Trends in molecular medicine *17*, 395-403.
Qin, H., and Powell-Coffman, J.A. (2004). The Caenorhabditis elegans aryl hydrocarbon receptor, AHR-1, regulates neuronal development. Developmental biology *270*, 64-75.
Rabinowitz, J.D., and Kimball, E. (2007). Acidic acetonitrile for cellular metabolome extraction from Escherichia coli. Analytical chemistry *79*, 6167-6173.
Sana, T., and Fischer, S. (2009). Lipidomics Discovery Profiling and Targeted LC/MS Analysis of 3T3-L1 Differentiating Adipocytes.
Schummer, C., Delhomme, O., Appenzeller, B.M., Wennig, R., and Millet, M. (2009). Comparison of MTBSTFA and BSTFA in derivatization reactions of polar compounds prior to GC/MS analysis. Talanta *77*, 1473-1482.
Semenza, G.L. (2002). HIF-1 and tumor progression: pathophysiology and therapeutics. Trends in molecular medicine *8*, S62-67.
Semple, R.K., Chatterjee, V.K., and O'Rahilly, S. (2006). PPAR gamma and human metabolic disease. The Journal of clinical investigation *116*, 581-589.
Suchorolski, M.T., Paulson, T.G., Sanchez, C.A., Hockenbery, D., and Reid, B.J. (2013). Warburg and Crabtree Effects in Premalignant Barrett's Esophagus Cell Lines with Active Mitochondria. PloS one *8*, e56884.
Tsumagari, K., Baribault, C., Terragni, J., Varley, K.E., Gertz, J., Pradhan, S., Badoo, M., Crain, C.M., Song, L., Crawford, G.E., *et al.* (2013). Early de novo DNA methylation and prolonged demethylation in the muscle lineage. Epigenetics : official journal of the DNA Methylation Society *8*, 317-332.
Turek-Plewa, J., and Jagodzinski, P.P. (2005). The role of mammalian DNA methyltransferases in the regulation of gene expression. Cellular & molecular biology letters *10*, 631-647.
Upadhyay, M., Samal, J., Kandpal, M., Singh, O.V., and Vivekanandan, P. (2013). The Warburg effect: Insights from the past decade. Pharmacology & therapeutics *137*, 318-330.
Warburg, O. (1956). On the origin of cancer cells. Science *123*, 309-314.
WormBase. WormBase Variation ju154. In WormBase Version: WS236 (US National Institutes of Health, British Medical Research Council).
Xiao, J.F., Zhou, B., and Ressom, H.W. (2012). Metabolite identification and quantitation in LC-MS/MS-based metabolomics. Trends in analytical chemistry : TRAC *32*, 1-14.
Xiong, N., Xiong, J., Jia, M., Liu, L., Zhang, X., Chen, Z., Huang, J., Zhang, Z., Hou, L., Luo, Z., *et al.* (2013). The role of autophagy in Parkinson's disease: rotenone-based modeling. Behavioral and brain functions : BBF *9*, 13.
Yan, X.J., Xu, J., Gu, Z.H., Pan, C.M., Lu, G., Shen, Y., Shi, J.Y., Zhu, Y.M., Tang, L., Zhang, X.W., *et al.* (2011). Exome sequencing identifies somatic mutations of DNA methyltransferase gene DNMT3A in acute monocytic leukemia. Nature genetics *43*, 309-315.
Yim, R.L., Kwong, Y.L., Wong, K.Y., and Chim, C.S. (2012). DNA Methylation of Tumor Suppressive miRNAs in Non-Hodgkin's Lymphomas. Frontiers in genetics *3*, 233.

Zhang, A., Sun, H., Wang, P., Han, Y., and Wang, X. (2012a). Modern analytical techniques in metabolomics analysis. The Analyst *137*, 293-300.
Zhang, B., Weng, Z., Sismanopoulos, N., Asadi, S., Therianou, A., Alysandratos, K.D., Angelidou, A., Shirihai, O., and Theoharides, T.C. (2012b). Mitochondria distinguish granule-stored from de novo synthesized tumor necrosis factor secretion in human mast cells. International archives of allergy and immunology *159*, 23-32.
Zhang, N. (2011). The role of endogenous aryl hydrocarbon receptor signaling in cardiovascular physiology. Journal of cardiovascular disease research *2*, 91-95.
Zhou, B., Xiao, J.F., Tuli, L., and Ressom, H.W. (2012). LC-MS-based metabolomics. Molecular bioSystems *8*, 470-481.